IEEE Access
Multidisciplinary | Rapid Review | Open Access Journal

Received December 6, 2020, accepted December 20, 2020, date of publication December 23, 2020, date of current version January 5, 2021.

Digital Object Identifier 10.1109/ACCESS.2020.3046910

Application of Dynamically Search Space Squeezed Modified Firefly Algorithm to a Novel Short Term Economic Dispatch of Multi-Generation Systems

SHEROZE LIAQUAT[1], MUHAMMAD SALMAN FAKHAR[2], SYED ABDUL RAHMAN KASHIF[2], AKHTAR RASOOL[3], OMER SALEEM[1], MUHAMMAD FAHAD ZIA[1], (Member, IEEE), AND SANJEEVIKUMAR PADMANABAN[4], (Senior Member, IEEE)

[1]Department of Electrical Engineering, National University of Computer and Emerging Sciences, Lahore 54000, Pakistan
[2]Department of Electrical Engineering, University of Engineering and Technology, Lahore 54000, Pakistan
[3]Department of Electrical Engineering, Sharif College of Engineering and Technology, Lahore 55150, Pakistan
[4]Department of Energy Technology, Aalborg University, 6700 Esbjerg, Denmark

Corresponding author: Sheroze Liaquat (shahroze.liaquat@nu.edu.pk)

ABSTRACT The absence of the global best component in the update equation of the conventional firefly algorithm degrades its exploration properties. This research proposes multi-update position criteria to enhance the exploration properties of the conventional firefly technique while including the effect of the global best solution on the movement of the fireflies in the search space of the objective function. Moreover, the dynamic search space squeezing is applied to constrict the movement of the fireflies within the certain limits to avoid their oscillatory movement as the solution approaches towards the global best by determining the optimal trajectory for each firefly. The robustness of the suggested firefly algorithm is tested on a hybrid energy system consisting of thermal, hydroelectric, and Photovoltaic (PV) energy source. The intermittent nature of the PV energy source is explained using fractional integral polynomial model and Auto Regressive Integrated Moving Average (ARIMA) model. The main dispatch problem is successfully computed using both the modified firefly and the simple firefly algorithm by determining the optimal power share of each energy source for different scheduling intervals. The suggested operational strategy reduces the overall generation cost of the system while preserving the various system constraints. Due to the stochastic nature of the meta-heuristic techniques, the two suggested algorithms are compared statistically for different test cases using the independent t-test results. The statistical comparison suggests that the performance of the modified firefly is superior to its conventional counterpart as the evaluation parameters of the modified firefly converge to relatively lower value as compared to the parameters of the simple firefly algorithm.

INDEX TERMS Modified firefly algorithm, auto regressive integrated moving average model, firefly algorithm, hybrid energy systems, independent t-test results.

I. INTRODUCTION

The distributed generation systems such as photovoltaic energy source and wind energy systems are now being extensively used with the conventional sources to meet the demand value over a particular scheduling interval [1]–[3]. The renewable energy systems do not have emission and environmental constraints and can be added to the conventional grid without having an adverse effect on the atmospheric conditions. The fundamental problem with such a dense power system having both conventional and non-conventional energy sources is to devise an efficient operational strategy to reduce the overall generation cost while meeting the system constraints. This constitutes a highly non-linear and non-convex optimization problem in the field of optimization theory [4]–[7]. The optimization problem dealing with

The associate editor coordinating the review of this manuscript and approving it for publication was Huaqing Li.

the optimal power scheduling of two major conventional sources, the hydroelectric source and the thermal energy source is known as the Short Term Hydro-Thermal Scheduling (STHTS) problem in literature. Several deterministic and heuristic techniques are suggested by the authors over the years to find the global optimum of the aforementioned problem [7], [8]. However, the addition of the distributed energy sources to the conventional grid requires more advanced optimization methods to efficiently solve the economic dispatch of the hybrid systems. Moreover, to handle the intermittent nature of the renewable energy sources and their dependence on the external atmospheric conditions, certain forecasting techniques are required to accurately predict the share of the renewable sources towards the economic dispatch.

A. RELEVANT LITERATURE

The work in [9] uses the non-linear programming to solve the non-convex hydro-thermal scheduling problem and compares its performance with the Cuckoo Search Algorithm (CSA), Particle Swarm Optimization (PSO) and Artificial Bee Colony (ABC) algorithm. The suggested non-linear programming method outperforms the mentioned algorithms by giving lower generation cost of the system for two test cases having different cost characteristics. The work in [10] proposes a hybrid ABC-BAT algorithm for solving the short term hydro thermal problem having multiple thermal units and compares its performance with the hybrid techniques like ABC-PSO and ABC-Quantum Evolutionary (ABC-QE) method. The suggested hybrid ABC-BAT algorithm outperforms the remaining hybrid techniques by giving lower mean generation cost. The work in [11] proposes a multi-objective economic emission dispatch problem having hydro and thermal generation sources and solves the suggested problem using the Multi-Objective Hybrid Grey Wolf Optimizer (MOHGWO). The suggested MOHGWO outperforms the MOHPSO and Nondominated Sorting Genetic Algorithm III (NSGA-III) by giving lower generation cost of the system. The work in [12] solves the hydro-thermal scheduling problem using the Lightning Attachment Procedure Optimization (LAPO) while considering the transmission losses and the valve point effect loading. The suggested LAPO surpasses the methods like Teaching Learning Based Optimization (TLBO) algorithm, PSO and the ABC algorithm. The work in [13] introduces a novel Crisscross Optimization (CSO) algorithm to solve the hydrothermal scheduling problem having multiple reservoirs connected in a cascade connection. The suggested CSO outperforms the techniques like Gravitational Search Algorithm (GSA), Differential Evolutionary (DE) Programming and PSO techniques. Similarly, the references [14]–[17] discuss the STHTS problem while using the different optimization techniques.

The references [9]–[17] discuss the optimal dispatch of a conventional STHTS problem using different meta-heuristic and deterministic methods. However, the addition of the renewable energy systems requires the upgradation of the optimization problem to include the effect of the distributed generation systems to the conventional grid. The work in [18] suggests the dispatch of a hybrid energy system consisting of wind, thermal and PV energy source. The authors consider the different modes for the dispatch problem such as the low emission mode, the energy saving mode and the high efficiency mode of operation for the suggested hybrid energy system. The work in [19] formulates a multi-objective economic emission dispatch problem for a hybrid energy system consisting of wind, PV, and hydro generation sources. The authors suggest a Multi-Objective Moth-Flame Optimization (MOMFO) technique to solve the proposed multi-objective optimization problem while using the IEEE 39-bus system. The work in [20] suggests a bi-level model for optimal scheduling of the renewable energy sources. The authors formulate an optimization problem while considering the planning and operational layers for the wind-solar system. The work in [21] suggests dynamic dispatch problem for system consisting of thermal, solar and wind energy sources while considering the underestimation and overestimation cost models for the distributed generation sources. The authors suggest an improved fireworks algorithm to solve the suggested dispatch problem. The references [22]–[26] also discuss the economic dispatch of a hybrid energy system consisting of both conventional and renewable energy sources.

B. RESEARCH GAP

The references [18]–[25] discuss the economic dispatch of the hybrid energy systems without providing any mathematical details for obtaining the used forecast results in their findings for distributed generation sources. The authors in [26] have suggested an efficient methodology to compute the solar forecast results, but their findings are limited to a single PV plant and total scheduling duration of nine hours. The firefly algorithm introduced in [26] to solve the economic dispatch of multi generation systems has poor global search mechanism which can result in the convergence of the algorithm towards local minimum. The firefly techniques introduced in [27], [28] consider the dynamic variation of the algorithm's parameters but the suggested techniques lack the exploration phase which can result in the premature convergence of the algorithm towards local optimum. The firefly technique discussed in [29] again uses the simple update criteria without considering the effect of the global best solution on the movement of remaining fireflies. The suggested firefly algorithm in [31] introduces a hybrid firefly-APSO algorithm to solve the dispatch problem, but the authors have not considered a balance relation between the exploration and exploitation phase, rather a simple global best term is introduced in addition to the local search. To introduce the global search for the conventional firefly technique, the authors in [34], [35] have introduced a firefly technique hybridized with the conventional PSO algorithm. Although, it is an efficient technique to solve the simple benchmark functions, but due to the complex structure of the two algorithms combined together, it will be highly inefficient for the large scale optimization problems

and can result in larger convergence time. Moreover, the above mentioned references have not considered an efficient strategy to keep the trajectory of the fireflies towards the global best value and avoid their oscillatory movement as the solution approaches towards the final value. Moreover, while comparing the different techniques suggested by the authors in [9]–[25], no statistical comparison is provided in order to statistically prove the significance of the suggested improved algorithm over the conventional techniques for a particular optimization problem. The authors in [26] have compared the suggested algorithms statistically using the independent t-test results, but their comparison study is limited to particular sample and population size.

C. MAJOR CONTRIBUTIONS

Based on the mentioned shortcomings of the literature, the **major contributions** of the suggested research are as follows:

1) A novel type of hydro-thermal-solar scheduling problem is proposed with multiple solar units and consideration of the intermittent nature of the solar energy source.
2) Introduce multi-update movement criteria for conventional firefly algorithm to balance its exploration and exploitation properties.
3) Introduce the concept of dynamic search space squeezing for conventional firefly technique to avoid the oscillatory movement of the fireflies.
4) A detailed design is proposed for forecasting the power share of the multiple PV plants of different rated capacity while considering the effect of the external atmospheric conditions on the performance of the PV module.
5) The proposed modified firefly algorithm is statistically compared with the conventional firefly technique while considering the effect of the sample size and population size on the convergence behavior of the algorithms.

The remaining paper is arranged as follows. The Section 2 provides the overview of the simple and modified firefly algorithm along with the suggested system configuration. The Section 3 discusses the complete design of the photovoltaic energy source. The Section 4 explains the methodology of the simple and modified firefly for the suggested dispatch problem along with the results for various test cases. The Section 5 compares the two algorithm statistically using the independent t-test results. The Section 6 highlights the major findings of the proposed research.

II. META-HEURISTIC OPTIMIZATION AND PROPOSED SYSTEM CONFIGURATION

Meta-heuristic optimization algorithms are gaining popularity in the domain of optimization theory as they are easier to implement as compared to the deterministic methods for finding the optimal solution of non-convex, highly non-linear, multi-modal, and complex objective functions. Moreover, the convergence of the meta-heuristic techniques towards the global optimum solution with lesser computational effort than the conventional methods like Gradient Search, Newton Raphson (NR) and Lagrange multiplier make them extremely useful to solve the various complex optimization problems. This research uses a modified firefly algorithm by suggesting parametric and structural changes in the conventional firefly technique. The firefly algorithm is selected over the other conventional meta-heuristic methods, as it is easier to execute for majority of the optimization problems and provides a good approximate of the global optimum solution [27]–[30].

A. CONVENTIONAL FIREFLY ALGORITHM

The flashing phenomenon of the fireflies in nature explains the basic working of the simple firefly algorithm. The light intensity/brightness of each firefly which depends upon the fitness value of the objective function dictates the movement of a lesser attractive firefly towards a brighter firefly. Each firefly represents a possible solution vector for the given optimization problem and the dimensions of each firefly are determined according to the decision variables of the objective function. The inverse square law as defined in (1) explains the dependence of the light intensity L at a distance r from the source.

$$L_r = \frac{L_s}{r^2} \tag{1}$$

where, L_r represents the light intensity evaluated at a distance r from the source. L_s shows the intensity of the source. To consider the effect of the medium on the intensity of the fireflies, the brightness value of the fireflies in terms of the medium's absorption coefficient δ is given by (2).

$$L = L_o e^{-\delta r} \tag{2}$$

where, L_o corresponds to the intensity of the fireflies at a distance $r = 0$ from the source. There exists a singular solution for $r = 0$ in (1), therefore in order to avoid the singularity, the above two equations can be combined to define the light intensity of the fireflies as follows:

$$L(r) = L_o e^{-\delta r^2} \tag{3}$$

The attractiveness of the fireflies β is directly proportional to the light intensity of the fireflies. Therefore, we can define the attractiveness value by the following relations:

$$\beta = \beta_o e^{-\delta r^2} \tag{4}$$

$$\beta = \frac{\beta_o}{1 + \delta r^2} \tag{5}$$

To compute the distance between the two fireflies a and b, following relations are used:

$$R_{ab} = \begin{cases} ((X_{a,1} - X_{b,1})^2 + (X_{a,2} - X_{b,2})^2)^{\frac{1}{2}}, & if\ D = 2 \\ \sqrt{\sum_{i=1}^{N} (X_{a,i} - X_{b,i})^2}, & if\ D = N \end{cases} \tag{6}$$

where, $X_{a,i}$ shows the *ith* component of the firefly a and $X_{b,i}$ represents the *ith* component of the firefly b. D represents the number of dimensions of each firefly. The following relation depicts the movement of a firefly a having lesser attractiveness value towards a brighter firefly b.

$$X_a = X_a + \underbrace{\beta_o e^{-\delta R_{ab}^2}(X_b - X_a)}_{\text{Influence of Neighbourhood Firefly}} + \underbrace{\alpha(rand - \frac{1}{2})}_{\text{Random Movement}} \tag{7}$$

where, α represents a number in the range [0,1] and rand shows the randomly generated numbers within the range [0,1]. The value of β_o can be taken equal to 1 for majority of the cases. The value of δ for most cases is given in the range [0.1,10] [32]. The pseudo code for the simple firefly algorithm is given as follows:

Function Pseudo Code for Simple Firefly Algorithm

```
Declare objective function f(X);
Declare constants α, δ, β_o and T;
Randomly initialize fireflies F;
Compute fitness value f(X_i), ∀ X_i ∈ F;
while t < T do
    for i ← 1 to N by 1 do
        for j ← 1 to N by 1 do
            Find R_ij using distance relation;
            if (L_j > L_i) then
                X_i ←
                X_i + β_o e^{-δR_ij^2}(X_j − X_i) + α(rand − 0.5);
    Determine f(X_i) at updated X_i, ∀ X_i ∈ F;
    Rank the fireflies according to their light
    intensity/fitness value;
    t ← t + 1;
Show the final results;
```

B. IMPROVED FIREFLY ALGORITHM

In conventional firefly algorithm, the parameters like α, β_o, δ are declared as constants, which can degrade the performance of the algorithm as the solution converges towards the global optimum. Moreover, the update equation as defined in (7) takes into account the influence of the brighter neighborhood firefly only, and the attractiveness of the global best firefly is not considered while updating the position of the fireflies in the search space of the objective function. This may result in the trapping of the solution towards the local optimum and can result in a larger convergence time. This research suggests the parametric modifications to make the parameters α, β_o, δ self-adaptive to accelerate the convergence of the algorithm towards the global optimum. Moreover, certain structural changes are suggested to include the influence of the global best firefly while updating the position of each firefly in order to balance the exploration and exploitation properties of each firefly. Then, the dynamic search space squeezing is implemented to preserve the oscillations of the fireflies in the search space of the objective function in order to improve the convergence value.

1) IMPROVEMENT 1: MAKING PARAMETRIC MODIFICATIONS

The randomization factor α, the medium's absorption coefficient δ and the attractiveness value at $r = 0$ (β_o) can be taken as self-adaptive quantities which accelerates the process of the convergence of the algorithm towards the global optimum solution. The modified values of the constants α, β_o and δ in accordance with [33] are given as follows:

$$\alpha = \alpha_o \theta^t \tag{8}$$

$$\beta_o = (\beta_{max} - \beta_{min})(\frac{t}{t_{max}})^2 + \beta_{min} \tag{9}$$

$$\delta = (\delta_{max} - \delta_{min})(\frac{t}{t_{max}})^2 + \delta_{min} \tag{10}$$

where, θ is in the range (0,1], α_o represents the initial randomization factor. β_{min} and β_{max} represent the minimum and maximum values for β_o. δ_{min} and δ_{max} represent the minimum and maximum values for the medium's absorption coefficient. t and t_{max} represent the current iteration and maximum number of iterations respectively. Equation (8) ensures that the random movement of the fireflies is restricted as the solution approaches towards the final value. Equation (9) ensures the attraction of the firefly i towards a brighter firefly j is within the certain controllable limits [β_{min} β_{max}]. Equation (10) controls the medium's absorption coefficient as the solution approaches towards the global optimum.

2) IMPROVEMENT 2: MAKING STRUCTURAL MODIFICATIONS

The simple firefly algorithm compares each firefly with the remaining fireflies and updates the position of each firefly having lesser intensity with respect to the brighter firefly. This results in larger convergence time as each firefly is compared with the remaining fireflies. It can also result in the convergence of the solution towards the local optimum and can increase the final converged fitness value. If the intensity of the global best firefly is included in (7) while updating the position of fireflies, then the convergence time can be reduced by a substantial factor. Moreover, it also ensures a balance between the exploration and exploitation properties of each firefly and prevents the convergence of the solution towards the local optimum [34], [35]. This research proposes a multi-update criteria for updating the position of each firefly to avoid their premature convergence and balance out the exploration and exploitation phases of the conventional firefly algorithm.

1) if the intensity of firefly i is less than j ($L_i < L_j$), then i will be attracted towards both j and global best firefly g^*.

$$X_i = X_i + \underbrace{c_1 \beta_o e^{-\delta R_{ij}^2}(X_j - X_i)}_{\text{Influence of Neighbourhood Firefly}} + \underbrace{\alpha(rand - \frac{1}{2})}_{\text{Random Movement}}$$

$$+ \underbrace{c_2\beta_o e^{-\delta R_{ig*}^2}(X_{g*} - X_i)}_{\text{Influence of Global Best Firefly}} \quad (11)$$

2) if the intensity of the firefly i is greater than j ($L_i > L_j$), then i will only be attracted towards the global best firefly g^*.

$$X_i = X_i + \underbrace{c_2\beta_o e^{-\delta R_{ig*}^2}(X_{g*} - X_i)}_{\text{Influence of Global Best Firefly}} + \underbrace{\alpha(rand - \frac{1}{2})}_{\text{Random Movement}} \quad (12)$$

where,

$$R_{ij} = \sqrt{\sum_{k=1}^{N}(X_{i,k} - X_{j,k})^2}, \; R_{ig^*} = \sqrt{\sum_{k=1}^{N}(X_{i,k} - X_{g^*,k})^2}$$

c_1 and c_2 given in the range [0,1] control the movement of firefly i towards the neighborhood firefly and the global best firefly respectively. R_{ij} and R_{ig^*} represent the distance between the firefly i with respect to firefly j and global best firefly g^*. Fig. (1) shows the vector representation for different modifications.

3) IMPROVEMENT 3: DYNAMIC SEARCH SPACE SQUEEZING

In conventional firefly technique, the search space is constrained by the maximum and minimum limits of the fireflies which remain same throughout the convergence process of the algorithm. This can result in the oscillations of the fireflies and can result in the divergence of the solution from the global optimum. One efficient method to keep the path of the fireflies towards the global solution is to dynamically squeeze the search space of the fireflies based on the global best firefly. This results in the transformation of the constraints from previous value to updated value after each iteration and maintains the trajectory of the fireflies towards the global optimum [36]. The equations (13)-(17) explain the procedure for dynamic search space squeezing.

$$\Delta_{lower,i}^{(t)} = \frac{X_{g*}^{(t)} - X_{i,min}^{(t)}}{X_{i,max}^{(t)} - X_{i,min}^{(t)}} \quad (13)$$

$$\Delta_{higher,i}^{(t)} = \frac{X_{i,max}^{(t)} - X_{g*}^{(t)}}{X_{i,max}^{(t)} - X_{i,min}^{(t)}} \quad (14)$$

$$\Delta_{lower,i}^{(t)} + \Delta_{higher,i}^{(t)} = 1 \quad (15)$$

$$X_{i,min}^{(t+1)} = X_{i,min}^{(t)} + (X_{g*}^{(t)} - X_{i,min}^{(t)})(\Delta_{lower,i}^{(t)}) \quad (16)$$

$$X_{i,max}^{(t+1)} = X_{i,max}^{(t)} + (X_{i,max}^{(t)} - X_{g*}^{(t)})(\Delta_{higher,i}^{(t)}) \quad (17)$$

where, $X_{i,min}^{(t)}$ and $X_{i,max}^{(t)}$ show the minimum and maximum limits of fireflies for iteration t. $X_{g*}^{(t)}$ shows the global best firefly for iteration t. $\Delta_{lower,i}^{(t)}$ and $\Delta_{higher,i}^{(t)}$ show the changing factor for maximum and minimum limits for iteration t. The pseudo code for the improved firefly algorithm incorporating the complete modifications is given as follows:

Function Pseudo Code for Improved Firefly Algorithm

```
Declare objective function f(X);
Declare constants
α_o, θ, β_max, β_min, δ_max, δ_min, t_max, c_1, c_2 ;
Randomly initialize fireflies F;
Compute fitness value f(X_i), ∀ X_i ∈ F;
Rank the fireflies and determine the initial global best
firefly X_g*;
while t < t_max do
    α ← α_o θ^t;
    β_o ← (β_max − β_min)(t/t_max)^2 + β_min;
    δ ← (δ_max − δ_min)(t/t_max)^2 + δ_min;
    for i ← 1 to N by 1 do
        for j ← 1 to N by 1 do
            Find R_ij using distance relation;
            Find R_ig* using distance relation;
            if (L_j > L_i) then
                X_i ← X_i + c_1 β_o e^{−δR_ij^2}(X_j − X_i) +
                c_2 β_o e^{−δR_ig*^2}(X_g* − X_i) +
                α(rand − 0.5);
            if (L_i > L_j) then
                X_i ← X_i + c_2 β_o e^{−δR_ig*^2}(X_g* −
                X_i) + α(rand − 0.5);
    Perform dynamic search space squeezing;
    Determine f(X_i) at updated X_i, ∀ X_i ∈ F;
    Rank the fireflies according to their light intensity;
    Determine the global best X_g* at updated X_i;
    t ← t + 1;
Show the final results;
```

C. SYSTEM MODEL

The proposed system consists of one hydro unit, one equivalent thermal energy source and three PV plants of different rated capacity. Fig. 2 shows the system configuration and the breakdown of the intervals for both cases. Two different test cases are developed in order to determine the robustness of the suggested firefly algorithm over the conventional technique. These test cases are developed according to the length of the scheduling problem and are given as follows:

1) The total scheduling period for case 1 is three consecutive days ($T = 72$ hours). Moreover, the total scheduling period is divided into six equal intervals ($n = 6$). Each interval is further divided into 12 sub intervals ($n_s = 12$), where each sub-interval is of equal duration (1 hour). The hydro power, thermal power and the load demand remain static for each main interval, whereas the solar power remains constant only for each sub interval. The product of the main intervals and the sub-intervals should be equal to the total length of the scheduling problem ($n \times n_s = T$).

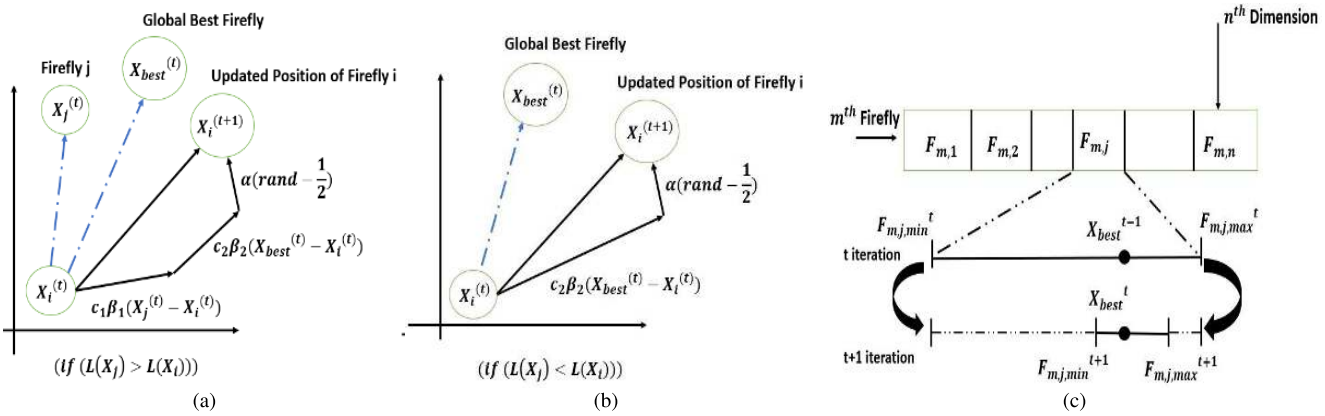

FIGURE 1. Vector representation for different modifications. (a) Structural modification (1). (b) Structural modification (2). (c) Dynamic search space squeezing.

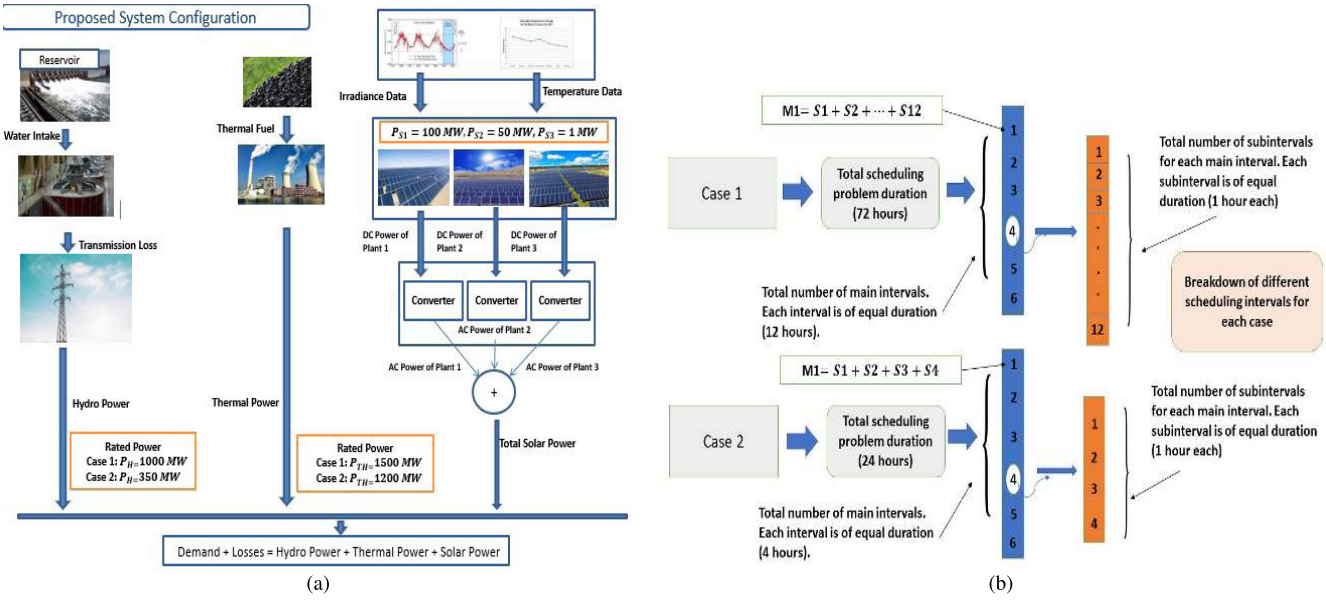

FIGURE 2. Model representation. (a) System configuration. (b) Breakdown of scheduling intervals.

2) The total scheduling period for case 2 spans over only a single day ($T = 24$ hours). Moreover, the total scheduling period is divided into six equal intervals ($n = 6$). Each interval is further divided into 4 sub intervals ($n_s = 4$), where each sub-interval is of equal duration (1 hour). The hydro power, thermal power and the load demand remain static for each main interval, whereas the solar power remains constant only for each sub interval. The product of the main intervals and the sub-intervals should be equal to the total length of the scheduling problem ($n \times n_s = T$).

III. DESIGN OF PHOTOVOLTAIC SYSTEM

The first step in solving the suggested dispatch problem is to forecast the solar power using the available data set. The work in [26] suggests an efficient method to compute the solar power results using the irradiance and temperature forecasts. This research extends the work in [26] to a system consisting of multiple PV plants and total scheduling problem of three days. The main steps to determine the solar power are, (i). Develop the mathematical model for single PV module. (ii). Forecast the irradiance and temperature levels. (iii). Using the suggested PV mathematical model and the forecast results, compute the solar power for different scheduling intervals.

A. MATHEMATICAL MODEL FOR PV MODULE

The two major parameters which determine the characteristics of the PV module are the irradiance and temperature levels. The suggested model determines the I-V characteristics and the power curves of the single PV module based on the temperature and irradiance values for different scheduling intervals [39]–[41]. The model presented in this research determines the current of the PV module as the function of

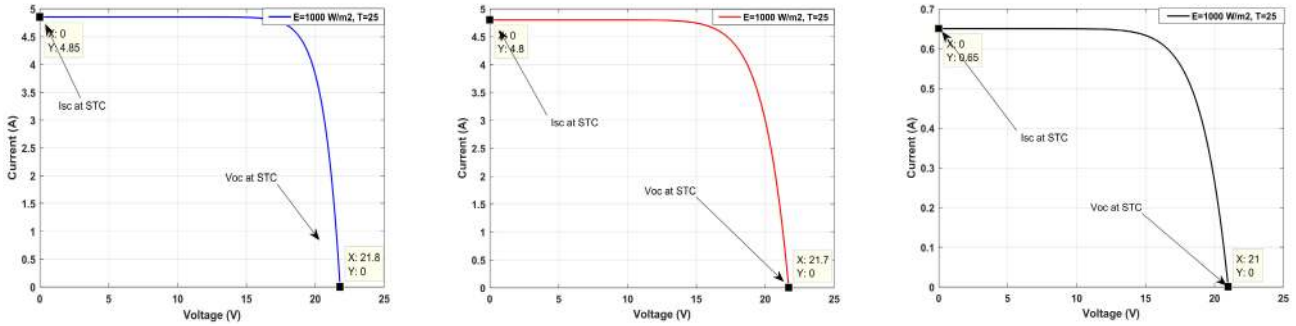

FIGURE 3. I-V characteristics of PV module at STC. (a) Plant 1. (b) Plant 2. (c) Plant 3.

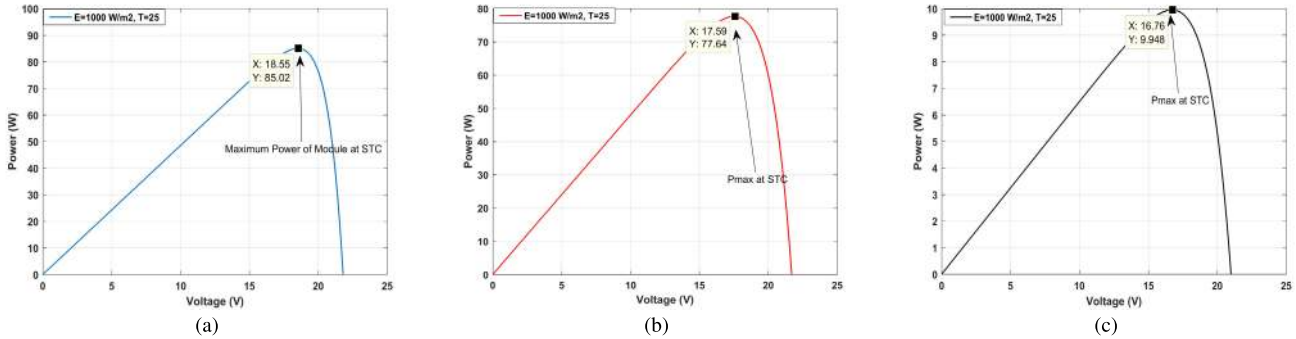

FIGURE 4. Power curve of PV module at STC. (a) Plant 1. (b) Plant 2. (c) Plant 3.

the module's voltage given as follows:

$$I(V) = I_s' - I_s' \left(\frac{V}{V_o'}\right)^{\alpha+\beta} \tag{18}$$

where, I_s' and V_o' represent the short circuit current and open circuit voltage of the module at arbitrary irradiance and temperature level. V represents the module's output voltage given in the range $[0, V_o']$. I represents the module's output current given in the range $[0, I_s']$. α represents a non-negative integer whereas, β shows an integer given in the range [0, 1]. The power of the module P is computed by the product of V and I and is given as follows:

$$P(V) = I(V).V = (I_s' - I_s' \left(\frac{V}{V_o'}\right)^{\alpha+\beta}) V \tag{19}$$

To determine the major parameters involved in (18), following set of equations are used:

$$V_o' = S_i.\frac{G}{G_{STC}}.T_{cv}.(T - T_{STC}) + V_{max} - (V_{max} - V_{min}).exp(\frac{G}{G_{STC}}.ln(\frac{V_{max} - V_o}{V_{max} - V_{min}})) \tag{20}$$

$$I_s' = P_i.\frac{G}{G_{STC}}.(I_s + T_{ci}.(T - T_{STC})) \tag{21}$$

$$\alpha + \beta = \frac{I_s}{I_s - I_{op}} \tag{22}$$

where, S_i and P_i represent the number of series connected and parallel connected modules respectively. G_{STC} and T_{STC} represent the irradiance and temperature values at STC. G and T are the arbitrary irradiance and temperature levels. V_{max} and V_{min} represent the maximum and minimum voltage levels of PV module. V_{op} and I_{op} represent the optimal voltage and current values of PV module. V_o and I_s represent the open circuit voltage and short circuit current at STC. T_{cv} and T_{ci} represent the temperature coefficients for V_o and I_s respectively.

1) VALIDATION OF SUGGESTED MODEL

The suggested system configuration consists of three different PV plants. The parameters of the single PV module are considered to be different for each plant in order to make the dispatch problem more practical. The characteristics of the PV module for each plant are listed in Table 1. Each module listed in Table 1 is tested at STC, variable irradiance conditions while keeping temperature constant and variable temperature levels while keeping irradiance constant. Fig. 3 shows the I-V characteristics of each module listed in Table 1 at STC. Fig. 4 shows the power curve of the modules at STC. At standard test conditions, the open circuit voltage, the short circuit current and the maximum power are equal to the rated values of Table 1. Fig. 5 and Fig. 6 show the effect of the variable irradiance levels on the I-V characteristics and the power curves of the module. The short circuit current and

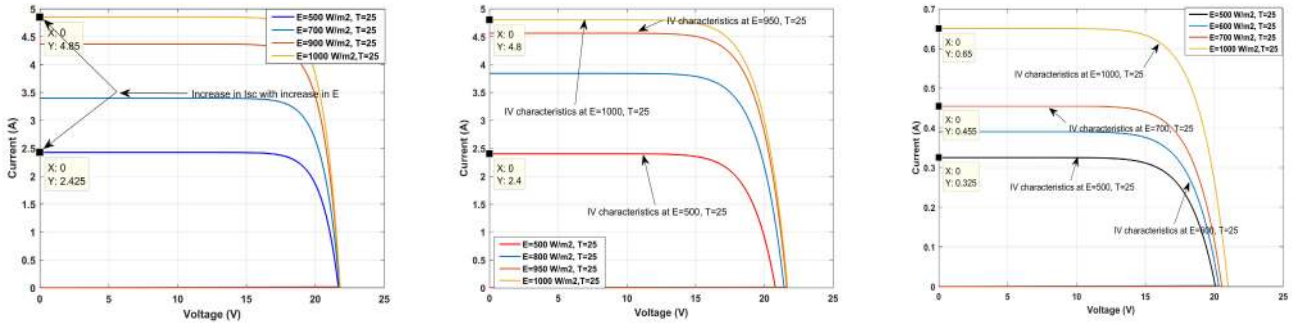

FIGURE 5. I-V characteristics at variable irradiance levels while keeping temperature constant. (a) Plant 1. (b) Plant 2. (c) Plant 3.

TABLE 1. Characteristics of single PV module for different plants in accordance with data provided in [41].

Plant Number	Module Type	Characteristics of PV Module							
		V_o (V)	I_s (A)	I_{op} (A)	V_{op} (V)	T_{cv} (V/°C)	T_{ci} (A/°C)	V_{max} (V)	P_{max} (W)
Plant 1	SQ80	21.8	4.85	4.58	17.5	-0.081	0.0014	21.810	85.02
Plant 2	SP75	21.7	4.80	4.40	17.0	-0.077	0.00206	22.243	77.64
Plant 3	SX-10	21.0	0.65	0.59	16.8	-0.080	0.0002	21.63	9.948

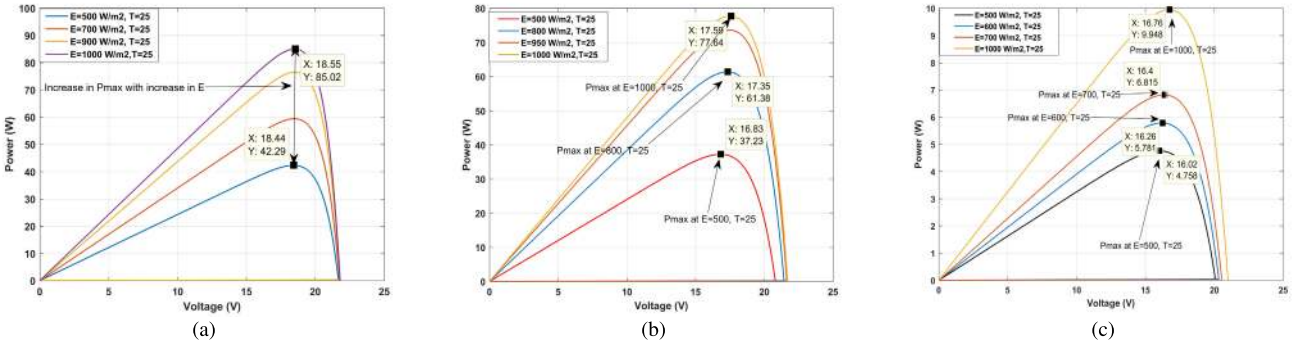

FIGURE 6. Power curves at variable irradiance levels while keeping temperature constant. (a) Plant 1. (b) Plant 2. (c) Plant 3.

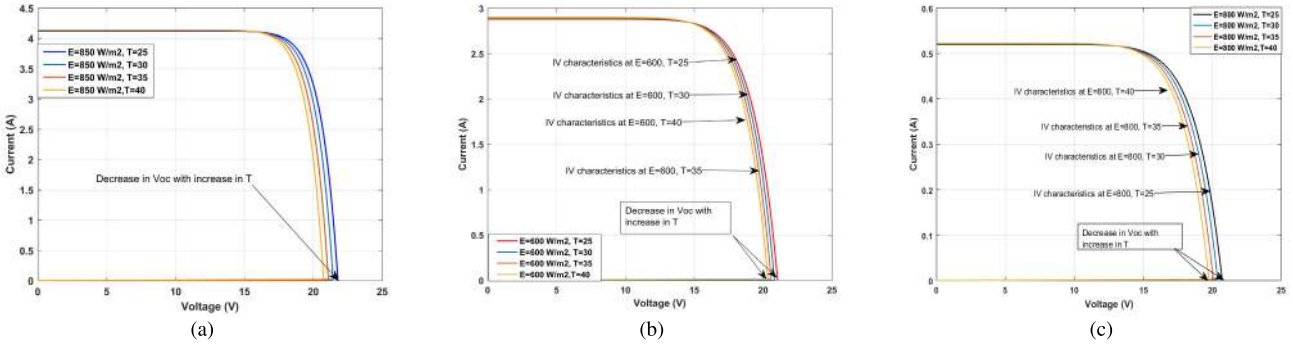

FIGURE 7. I-V characteristics at variable temperature levels while keeping irradiance constant. (a) Plant 1. (b) Plant 2. (c) Plant 3.

the maximum power of the module increases at the elevated irradiance levels while keeping temperature constant. Fig. 7 and Fig. 8 show the effect of the elevated temperature levels on the I-V characteristics and the power curves of the module while keeping irradiance constant. The open circuit voltage and the maximum power of the module decreases at the higher temperature levels while keeping irradiance constant.

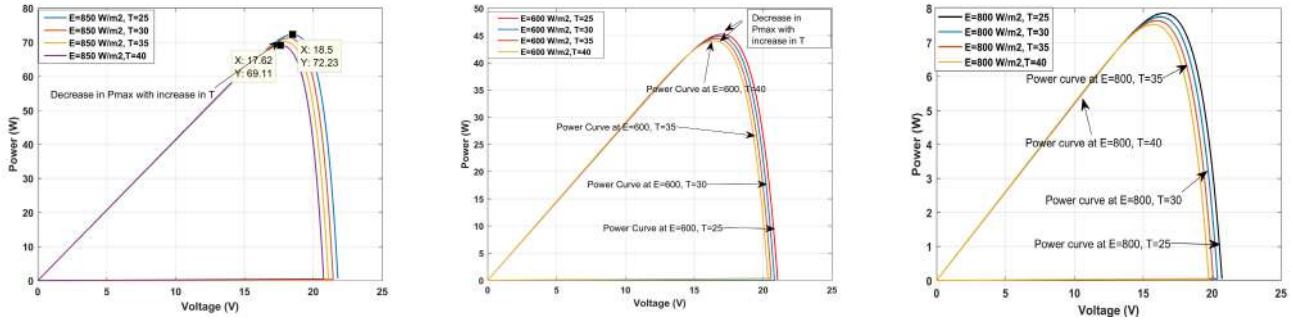

FIGURE 8. Power curves at variable irradiance levels while keeping temperature constant. (a) Plant 1. (b) Plant 2. (c) Plant 3.

B. FORECASTING OF IRRADIANCE AND TEMPERATURE LEVELS

The mathematical model described previously depends upon the two major input parameters, the irradiance, and the temperature levels. Therefore, the next step in the design of the photovoltaic system is to forecast the desired parameters for the entire scheduling problem. The first test case spans over a duration of three days, therefore in order to compute the solar power share, the forecasted irradiance and temperature levels are required for three consecutive days. For case 2, this research uses the forecasted values of temperature and irradiance computed at day one of the case 1.

1) BOX JENKINS MODEL

An efficient technique described in the literature to compute the time series forecasts of the non-stationary dataset is the Box-Jenkins methodology [42]–[44]. Box-Jenkins methodology describes the method to compute the optimal parameters of the auto-regressive integrated moving average model. The three main parameters of the ARIMA model are the order of the Auto-Regressive model defined by the variable p, the order of the Moving Average (MA) model defined by the variable q, and the differentiating order defined by the variable d. The mathematical relations for the AR, MA and ARMA models are defined as follows:

$$X_t = \begin{cases} \alpha + \sum_{n=1}^{p} \theta_n X_{t-n} + \epsilon_t, & if\ q = 0,\ p > 0 \\ \epsilon_t + \sum_{n=1}^{q} \delta_n \epsilon_{t-n}, & if\ q > 0,\ p = 0 \\ \alpha + \epsilon_t + \sum_{n=1}^{p} \theta_n X_{t-n} & if\ q > 0,\ p > 0 \\ \quad + \sum_{n=1}^{q} \delta_n \epsilon_{t-n} & \end{cases} \tag{23}$$

By including the lag operator ($L^k(X_t) = X_{t-k}$), the above set of equations can be written as follows:

$$\epsilon_t = (1 - \sum_{n=1}^{p} \theta_n L^n) X_t = \theta_p(L) X_t \tag{24}$$

$$X_t = (1 + \sum_{n=1}^{q} \delta_n L^n) \epsilon_t = \delta_q(L) \epsilon_t \tag{25}$$

$$(1 - \sum_{n=1}^{p} \theta_n L^n) X_t = (1 + \sum_{n=1}^{q} \delta_n L^n) \epsilon_t \tag{26}$$

The ARIMA(p,d,q) model can be defined as follows:

$$(1 - \sum_{n=1}^{p} \theta_n L^n)(1 - L^d) X_t = (1 + \sum_{n=1}^{q} \delta_n L^n) \epsilon_t \tag{27}$$

where, $\theta_1, \theta_2, \ldots, \theta_n$ represent the parameters of auto-regressive model. $\delta_1, \delta_2, \ldots, \delta_n$ represent the parameters of moving-average model. $\epsilon_t, \epsilon_{t-1}, \ldots, \epsilon_{t-n}$ define the white noise terms.

2) EXAMPLE

The major steps involved in producing the time series forecasts using the ARIMA model are the (i). Identification of the model. (ii). Estimation of the parameters. (iii). Residual diagnostics. The dataset obtained from the National Renewable Energy Laboratory Website (NREL) [45] includes the daily irradiance and temperature curves for the year 2015. The irradiance and the temperature data set are plotted in the Fig. 9. In order to find the optimal parameters p, d and q of the ARIMA model for the given data set, the readers are encouraged to go through the detailed steps and the analysis described in [26]. For the sake of the simplicity of the readers, the steps of the Box-Jenkins methodology are skipped for the given data set and the final forecast results for both irraidance and temperature curves for three consecutive days (December 22, 2015- December 25, 2015) are shown in the Fig. 10.

C. PV POWER COMPUTATION USING DEVELOPED MODEL AND FORECASTED PARAMETERS

In order to determine the PV power for three consecutive days, the forecasted irradiance and temperature levels and mathematical model developed previously are used while taking into account the following assumptions.

1) The irradiance and temperature values remain constant for each sub interval (1 hour) and changes at the beginning of the next sub-interval.
2) The power of the module for each sub-interval is computed using the mathematical model and the forecasted parameters for that interval.

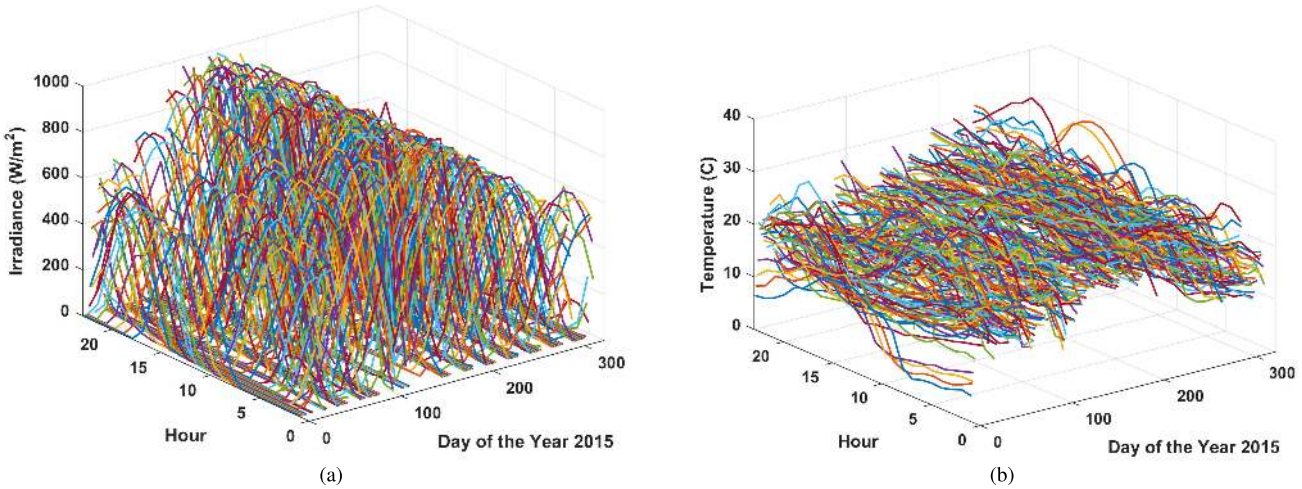

(a) (b)

FIGURE 9. Data set obtained from NREL website for the year 2015. (a) Irradiance data. (b) Temperature data.

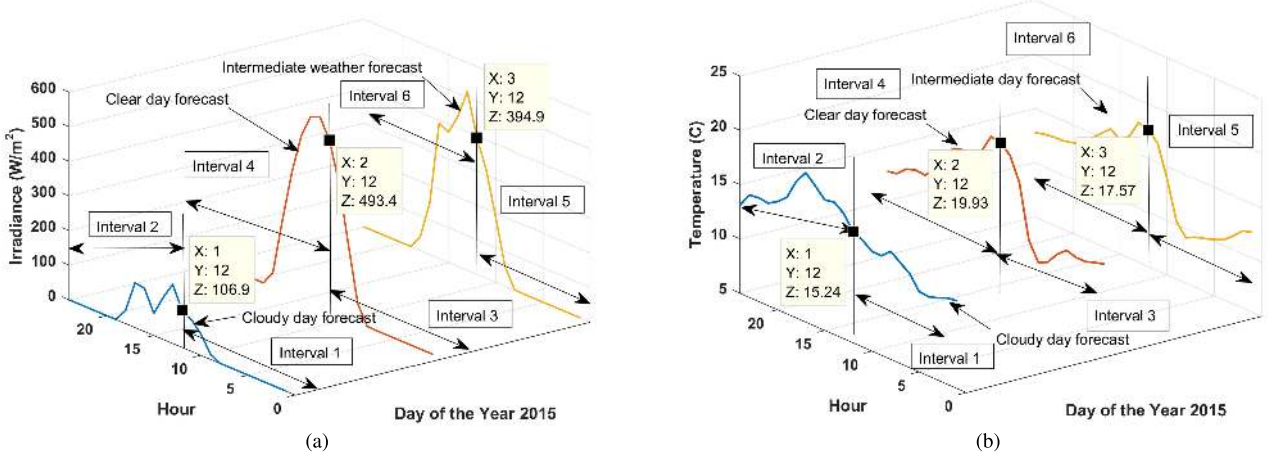

(a) (b)

FIGURE 10. Forecast results obtained for three consecutive days (December 22, 2015- December 25, 2015). (a) Irradiance forecast. (b) Temperature forecast.

3) The maximum power point condition is used while computing the power of each module.
4) The total DC power of the PV plant is given by the sum of the maximum power of all the modules for the given sub-interval.
5) The AC power of the plant is computed by the product of the DC power and the converter's efficiency.
6) The total number of the modules required are according to the rated system capacity of each plant.

Table 2 summarizes different parameters for each plant. Table 3 summarizes the forecast results for day 1. Table 4 summarizes the forecast results for day 2. Table 5 summarizes the forecast results for day 3. Table 6 summarizes the total power contribution of each plant for different scheduling intervals for case 1 (December 22, 2015-December 25, 2015). Table 7 summarizes the total power contribution of each plant for different scheduling intervals for case 2 (December 22, 2015). For case 1, the total power for each interval is equal to the sum of the power contribution of 12 sub-intervals (12 hours). For case 2, the total power for each interval is equal to the sum of the power contribution of 4 sub-intervals (4 hours). This completes the forecast results of PV system for different cases. The next section describes the overall methodology and the problem formulation for the given optimization problem along with the results of each case.

IV. METHODOLOGY AND RESULTS

The objective function of the conventional hydrothermal scheduling problem minimizes the total fuel cost of the thermal generation while preserving the reservoir and thermal constraints [46]–[48]. This sections describes the updated hydro-thermal-solar scheduling problem and presents the optimal power allocation of each energy source for different test cases while meeting the different system constraints.

A. PROBLEM FORMULATION

The objective function for the considered dispatch problem which aims to reduce the thermal cost of the system can be

TABLE 2. System parameters for each PV plant.

Plant Number	Module Type	System Parameters			
		P_{max} (W)	Rated System Capacity (S) (MW)	Number of Modules $N_m = \frac{S}{P_{max}}$	Converter's Efficiency (%)
Plant 1	SQ80	85.02	100	1176194	95
Plant 2	SP75	77.64	50	643998	95
Plant 3	SX-10	9.948	1	100523	95

TABLE 3. PV power computation for day 1 having cloudy conditions (December 22, 2015).

Scheduling Interval	Day Hour	Forecasted Parameters		Plant 1			Plant 2			Plant 3		
		Irradiance (W/m^2)	Temperature (°C)	P_{max} (W)	P_{DC} (MW)	P_{AC} (MW)	P_{max} (W)	P_{DC} (MW)	P_{AC} (MW)	P_{max} (W)	P_{DC} (MW)	P_{AC} (MW)
Interval 1	12:00–1:00	0.081	13.06	0.0064	0.0075	0.0072	0.0054	0.0034	0.0032	0.0007	0.000069	0.000065
	1:00–2:00	0.102	12.94	0.0080	0.0094	0.0089	0.0067	0.0043	0.0040	0.0009	0.000086	0.000082
	2:00–3.00	0.098	12.56	0.0078	0.0091	0.0086	0.0065	0.0041	0.0039	0.0008	0.000083	0.000079
	3:00–4:00	0.102	12.29	0.0080	0.0094	0.0089	0.0067	0.0043	0.0040	0.0009	0.000086	0.000082
	4:00–5:00	0.10	12.40	0.0079	0.0092	0.0088	0.0066	0.0042	0.0040	0.0008	0.000085	0.000080
	5:00–6:00	0.090	13.66	0.0071	0.0083	0.0079	0.0059	0.0038	0.0036	0.0008	0.000076	0.000072
	6:00–7:00	0.083	14.29	0.0066	0.0077	0.0073	0.0055	0.0035	0.0033	0.0007	0.000070	0.000067
	7:00–8:00	0.181	14.95	0.0143	0.016	0.015	0.011	0.0076	0.0072	0.0015	0.00015	0.00014
	8:00–9:00	15.37	14.16	1.218	1.433	1.36	1.017	0.65	0.62	0.1304	0.0131	0.0124
	9:00–10:00	61.26	14.18	4.93	5.80	5.51	4.129	2.65	2.52	0.5292	0.053	0.050
	10:00–11:00	91.36	14.83	7.42	8.73	8.29	6.229	4.01	3.81	0.798	0.080	0.076
	11:00–12:00	106.94	15.23	8.72	10.26	9.75	7.33	4.72	4.48	0.939	0.094	0.089
Interval 2	12:00–1:00	170.65	16.55	14.12	16.60	15.77	11.94	7.69	7.30	1.52	0.153	0.146
	1:00–2:00	121.24	17.2	9.92	11.67	11.09	8.35	5.37	5.11	1.06	0.107	0.102
	2:00–3:00	63.78	17.02	5.14	6.04	5.74	4.30	2.77	2.63	0.55	0.055	0.052
	3:00–4:00	125.17	17.92	10.25	12.06	11.46	8.63	5.56	5.28	1.105	0.111	0.105
	4:00–5:00	128.90	18.76	10.56	12.43	11.81	8.90	5.73	5.44	1.139	0.114	0.108
	5:00–6:00	37.84	17.60	3.02	3.55	3.38	2.52	1.629	1.54	0.324	0.0325	0.030
	6:00–7:00	0.360	15.73	0.028	0.033	0.031	0.02	0.015	0.014	0.0030	0.00030	0.00029
	7:00–8:00	0.014	14.95	0.0012	0.0013	0.0012	0.0010	0.00062	0.00059	0.0001	0.000012	0.000011
	8:00–9:00	0.030	14.42	0.0024	0.0028	0.0027	0.0020	0.0013	0.0012	0.0003	0.000026	0.000024
	9:00–10:00	0.064	14.54	0.0051	0.0060	0.0057	0.0043	0.0027	0.0026	0.0005	0.000054	0.000052
	10:00–11:00	0.061	14.41	0.0049	0.0057	0.0054	0.0041	0.0026	0.0024	0.0005	0.000052	0.000049
	11:00–12:00	0.038	13.08	0.0030	0.0035	0.0033	0.0025	0.0016	0.0015	0.0003	0.000032	0.000031

written as follows:

$$min(f) = \sum_{j=1}^{N_S} n_j F(P_{TH,j}) \tag{28}$$

where, n_j represents the total hours of each scheduling interval. $F(P_{TH,j})$ represents the cost function of the thermal generation for particular scheduling interval j. N_S represents the total number of scheduling intervals. The total cost of the system including the PV cost is given as follows:

$$F_T = F(P_T) + C_{1,s} \sum_{j=1}^{N_S} P_{S_{1,f,j}} + C_{2,s} \sum_{j=1}^{N_S} P_{S_{2,f,j}} + C_{3,s} \sum_{j=1}^{N_S} P_{S_{3,f,j}} \tag{29}$$

where, F_T represents the total cost of the system. $F(P_T)$ represents the total converged thermal cost of the system. $C_{1,s}$, $C_{2,s}$ and $C_{3,s}$ represent the cost coefficients given in \$/kWh for PV plant 1, 2 and 3 respectively. $P_{S_{1,f,j}}$, $P_{S_{2,f,j}}$ and $P_{S_{3,f,j}}$ represent the forecasted solar power for particular scheduling interval j for PV plant 1, 2 and 3 respectively. The defined objective function is subjected to following constraints.

1) POWER BALANCE CONSTRAINT

The sum of the power contribution from the thermal energy source, the hydro source and all three PV plants for a particular scheduling interval must be equal to the demand plus the transmission losses for that interval.

$$P_{H,j} + P_{TH,j} + \sum_{i=1}^{N_{sp}} P_{S_{i,j}} = P_{D,j} + P_{L,j} \tag{30}$$

TABLE 4. PV power computation for day 2 having clear sky conditions (December 23, 2015).

Scheduling Interval	Day Hour	Forecasted Parameters		Plant 1			Plant 2			Plant 3		
		Irradiance (W/m^2)	Temperature (°C)	P_{max} (W)	P_{DC} (MW)	P_{AC} (MW)	P_{max} (W)	P_{DC} (MW)	P_{AC} (MW)	P_{max} (W)	P_{DC} (MW)	P_{AC} (MW)
Interval 3	12:00–1:00	0.057	12.93	0.0046	0.0053	0.0050	0.0038	0.0024	0.0023	0.0005	0.000049	0.000046
	1:00–2:00	0.054	12.69	0.0043	0.0050	0.0047	0.0036	0.0022	0.0021	0.0005	0.000045	0.000043
	2:00–3.00	0.039	12.41	0.0031	0.0036	0.0034	0.0026	0.0016	0.0015	0.0003	0.000033	0.000031
	3:00–4:00	0.068	12.39	0.0054	0.0063	0.0060	0.0045	0.0029	0.0027	0.0006	0.000058	0.000055
	4:00–5:00	0.062	12.67	0.0049	0.0057	0.0055	0.0041	0.0026	0.0025	0.0005	0.000053	0.000050
	5:00–6:00	0.043	11.94	0.0034	0.0040	0.0038	0.0028	0.0018	0.0017	0.0004	0.000036	0.000034
	6:00–7:00	0.034	10.82	0.0027	0.0031	0.0029	0.0022	0.0014	0.0013	0.0003	0.000028	0.000027
	7:00–8:00	1.233	10.41	0.0971	0.114	0.108	0.0810	0.0521	0.049	0.0104	0.00104	0.00092
	8:00–9:00	55.90	12.07	4.49	5.287	5.022	3.759	2.420	2.29	0.481	0.048	0.046
	9:00–10:00	215.15	16.98	17.93	21.09	20.04	15.251	9.821	9.33	1.95	0.196	0.186
	10:00–11:00	381.14	19.13	32.29	37.98	36.08	28.03	18.05	17.15	3.58	0.36	0.34
	11:00–12:00	493.37	19.92	42.04	49.45	46.98	36.95	23.80	22.61	4.72	0.47	0.45
Interval 4	12:00–1:00	548.54	20.10	46.84	55.10	52.34	41.41	26.66	25.33	5.300	0.53	0.50
	1:00–2:00	537.99	18.41	46.06	54.17	51.46	40.66	26.18	24.87	5.206	0.52	0.49
	2:00–3:00	470.73	17.56	40.20	47.29	44.92	35.24	22.69	21.56	4.512	0.45	0.43
	3:00–4:00	352.82	17.73	29.87	35.13	33.37	25.83	16.63	15.80	3.306	0.33	0.31
	4:00–5:00	203.30	17.48	16.91	19.89	18.89	14.36	9.248	8.78	1.837	0.18	0.17
	5:00–6:00	42.44	16.35	3.39	3.99	3.79	2.841	1.829	1.73	0.364	0.036	0.034
	6:00–7:00	0.551	14.81	0.043	0.051	0.048	0.036	0.023	0.022	0.0046	0.00046	0.00044
	7:00–8:00	0.047	13.87	0.0037	0.0043	0.0041	0.0031	0.0019	0.0018	0.0004	0.000039	0.000037
	8:00–9:00	0.027	13.96	0.0021	0.0025	0.0023	0.0018	0.0011	0.0010	0.0002	0.000022	0.000021
	9:00–10:00	0.073	13.67	0.0058	0.0067	0.0064	0.0048	0.0031	0.0029	0.0006	0.000062	0.000059
	10:00–11:00	0.081	12.87	0.0064	0.0075	0.0071	0.0053	0.0034	0.0032	0.0007	0.000068	0.000065
	11:00–12:00	0.069	12.70	0.0055	0.0064	0.0061	0.0046	0.0029	0.0027	0.0006	0.000058	0.000055

where, $P_{H,j}$, $P_{TH,j}$, $P_{D,j}$ and $P_{L,j}$ represent the hydro power, thermal power, the demand value and the transmission losses for a particular scheduling interval j. N_{sp} represents the total number of PV plants. $P_{S_{i,j}}$ represents the contribution of the i^{th} PV plant for particular scheduling interval j.

2) POWER LIMITS CONSTRAINT

The hydro power and the thermal power must be within the maximum and minimum power limits. The solar power must be equal to the forecasted value for particular scheduling interval j. The following equality and inequality constraints are defined for different sources.

$$P_{S_{1,j}} = P_{S_{1,f,j}} \tag{31}$$

$$P_{S_{2,j}} = P_{S_{2,f,j}} \tag{32}$$

$$P_{S_{3,j}} = P_{S_{3,f,j}} \tag{33}$$

$$P_{H,min} \leq P_{H,j} \leq P_{H,max} \tag{34}$$

$$P_{TH,min} \leq P_{TH,j} \leq P_{TH,max} \tag{35}$$

where, $P_{TH,min}$, $P_{TH,max}$ represents the thermal power limits. $P_{H,min}$, $P_{H,max}$ represents the hydro power limits.

3) RESERVOIR CONSTRAINTS

The volume of the reservoir for a particular scheduling interval must be within the maximum and minimum values given as follows:

$$V_{min} \leq V_j \leq V_{max} \tag{36}$$

where, V_{min} and V_{max} are the minimum and maximum limits of the volume. V_j represents the volume of the reservoir for a particular scheduling interval j. Moreover, the initial and final volume of the reservoir must be equal to the desired parameters given as follows:

$$V_o = V_{initial} \tag{37}$$

$$V_1 = V_{final} \tag{38}$$

where, $V_{initial}$ and V_{final} represent the desired initial and final volume of the reservoir. Finally, the discharge rate constraints are given as follows:

$$Dis_{min} \leq D_j \leq Dis_{max} \tag{39}$$

$$\sum_{j=1}^{N_S} n_j Dis_j = Dis_t \tag{40}$$

where, Dis_{min} and Dis_{max} represent the minimum and maximum discharge rate limits. D_j represents the discharge rate for a particular scheduling interval j.

4) EQUATION OF CONTINUITY

The volume of the reservoir and the discharge rate must be related by the equation of continuity given as follows:

$$V_j = V_{j-1} + n_j(I_{f,j} - Dis_j - S_{p,j}) \tag{41}$$

where, $I_{f,j}$ and $S_{p,j}$ represent the inflow and the spillage of the water for the particular scheduling interval j.

TABLE 5. PV power computation for day 3 having intermediate weather conditions (December 24, 2015).

Scheduling Interval	Day Hour	Forecasted Parameters		Plant 1			Plant 2			Plant 3		
		Irradiance (W/m^2)	Temperature (°C)	P_{max} (W)	P_{DC} (MW)	P_{AC} (MW)	P_{max} (W)	P_{DC} (MW)	P_{AC} (MW)	P_{max} (W)	P_{DC} (MW)	P_{AC} (MW)
Interval 5	12:00–1:00	0.065	12.366	0.0052	0.0068	0.0057	0.0043	0.0027	0.0026	0.0006	0.000055	0.000052
	1:00–2:00	0.065	12.09	0.0052	0.0060	0.0057	0.0043	0.0027	0.0026	0.0006	0.000055	0.000052
	2:00–3.00	0.065	11.22	0.0052	0.0060	0.0057	0.0043	0.0027	0.0026	0.0006	0.000055	0.000052
	3:00–4:00	0.074	10.51	0.0058	0.0068	0.0065	0.0049	0.0031	0.0029	0.0006	0.000062	0.000059
	4:00–5:00	0.032	10.15	0.0026	0.0030	0.0028	0.0021	0.00137	0.00130	0.0003	0.000027	0.000026
	5:00–6:00	0	9.863	0	0	0	0	0	0	0	0	0
	6:00–7:00	0.038	9.61	0.0030	0.0035	0.0034	0.0025	0.0016	0.0015	0.0003	0.000032	0.000031
	7:00–8:00	1.44	9.17	0.1139	0.134	0.127	0.095	0.061	0.058	0.0122	0.0012	0.0011
	8:00–9:00	55.93	10.30	4.496	5.28	5.02	3.75	2.42	2.30	0.4821	0.0484	0.0460
	9:00–10:00	188.08	13.90	15.62	18.38	17.46	13.24	8.52	8.10	1.695	0.170	0.161
	10:00–11:00	313.0	16.76	26.42	31.07	29.52	22.74	14.64	13.91	2.91	0.292	0.277
	11:00–12:00	394.92	17.57	33.55	39.47	37.49	29.16	18.78	17.84	3.73	0.375	0.356
Interval 6	12:00–1:00	517.08	17.87	44.26	52.06	49.45	38.98	25.10	23.85	4.992	0.50	0.47
	1:00–2:00	434.76	16.22	37.11	43.65	41.47	32.40	20.86	19.82	4.14	0.417	0.396
	2:00–3:00	376.17	15.58	31.98	37.62	35.74	27.73	17.86	16.96	3.55	0.356	0.339
	3:00–4:00	391.23	16.14	33.29	39.15	37.19	28.91	18.62	17.69	3.70	0.372	0.353
	4:00–5:00	148.04	15.34	12.19	14.34	13.63	10.29	6.62	6.29	1.31	0.132	0.125
	5:00–6:00	40.95	14.51	3.27	3.85	3.66	2.73	1.76	1.67	0.35	0.035	0.033
	6:00–7:00	0.191	13.62	0.015	0.017	0.016	0.012	0.0081	0.0077	0.0016	0.00016	0.00015
	7:00–8:00	0.068	13.34	0.0054	0.0063	0.0060	0.0045	0.0029	0.0027	0.0006	0.000058	0.000055
	8:00–9:00	0.064	13.15	0.0050	0.0059	0.0056	0.0042	0.0027	0.0025	0.0005	0.000054	0.000051
	9:00–10:00	0.084	13.11	0.0066	0.0077	0.0074	0.0055	0.0035	0.0033	0.0007	0.000071	0.000067
	10:00–11:00	0.078	12.99	0.0061	0.0072	0.0068	0.0051	0.0032	0.0031	0.0007	0.000066	0.000062
	11:00–12:00	0.0155	12.76	0.0012	0.0014	0.0013	0.0010	0.00065	0.00062	0.0001	0.000013	0.000012

TABLE 6. Total AC power contribution of each plant for different scheduling intervals for case 1 (December 22, 2015-December 25, 2015). Each scheduling interval is of equal duration (12 hours).

Plant Number	Total AC Power for Different Scheduling Intervals (MW)					
	Interval 1	Interval 2	Interval 3	Interval 4	Interval 5	Interval 6
Plant 1	25.0000	59.3187	108.2738	204.8946	89.6708	181.2119
Plant 2	11.479	27.351	51.456	98.1430	42.2326	86.3303
Plant 3	0.229553	0.546556	1.027858	1.961098	0.843884	1.725499

TABLE 7. Total AC power contribution of each plant for different scheduling intervals for case 2 (December 22, 2015). Each scheduling interval is of equal duration (4 hours).

Plant Number	Total AC Power for Different Scheduling Intervals (MW)					
	Interval 1	Interval 2	Interval 3	Interval 4	Interval 5	Interval 6
Plant 1	0.034	0.040	24.926	44.077	15.224	0.017
Plant 2	0.015	0.018	11.446	20.334	7.009	0.008
Plant 3	0.00031	0.00037	0.022888	0.040634	0.014006	0.00016

B. STEPS OF IMPROVED FIREFLY

In order to solve the suggested dispatch problem, the steps of only improved firefly algorithm are highlighted for the sake of the simplicity of the readers. These are given as follows:

1) Find the irradiance and temperature forecast results for the desired scheduling period.
2) Using the mathematical model described in Section 3 and the forecast results, compute the PV power share for each plant for different scheduling intervals.
3) Declare constants like α_o, θ, β_{max}, β_{min}, δ_{max}, δ_{min},t_{max},c_1, c_2.
4) Randomly initialize the volume vectors as fireflies for all scheduling intervals and check the volume

TABLE 8. Different parameters for each case.

Case Number	Parameter Type									
	V_{max} (acre-ft)	V_{min} (acre-ft)	$V_{initial}$ (acre-ft)	V_{final} (acre-ft)	I_f (acre-ft/hr)	S_p (acre-ft/hr)	n (hr)	$C_{1,s}$ ($/kWhr)	$C_{2,s}$ ($/kWhr)	$C_{3,s}$ ($/kWhr)
Case 1	100,000	60,000	124,000	60,000	2000	0	12	0.120	0.150	0.120
Case 2	12000	18000	16000	12000	2000	0	4	0.120	0.150	0.120

constraints. The volume vector for a particular iteration t and firefly F is given as follows:

$$\mathbf{V}_F^{(t)} = \begin{bmatrix} V_{1,F}^{(t)} & V_{2,F}^{(t)} & V_{3,F}^{(t)} & \cdots\cdots & V_{N_S,F}^{(t)} \end{bmatrix}^{\mathbf{T}}$$

5) Determine the initial global best firefly. The initial global best firefly corresponds towards the volume vector which has the minimum thermal cost for the initially generated volume vectors.
6) Determine the discharge rate vector using the volume vectors and check the discharge rate constraint. The discharge rate for particular iteration t, scheduling interval j and firefly F is computed using the equation of continuity defined in (41) and is given as follows:

$$= \begin{cases} \dfrac{(V_o - V_{1,F}^{(t)})}{n_1} & if\ j = 1 \\ \dfrac{(V_{j-1,F}^{(t)} - V_{j,F}^{(t)})}{n_j} + (I_{f,j} - S_{p,j}) & if\ j \neq 1 \end{cases}$$
$$\forall\, j \in \{1, 2, 3, \ldots, N_S\}$$

7) Determine the hydro power using the discharge rate for each scheduling interval and check the hydro power limit constraint. The hydro power vector is computed as the function of the discharge rate and is given as follows:

$$\mathbf{P}_{H\,(N_S\times 1)}^{(t)} = \mathbf{func}(\mathbf{Dis}^{(t)}) = \begin{bmatrix} \mathbf{func}(Dis_{1,F}^{(t)}) \\ \mathbf{func}(Dis_{2,F}^{(t)}) \\ \mathbf{func}(Dis_{3,F}^{(t)}) \\ . \\ . \\ . \\ \mathbf{func}(Dis_{N_S,F}^{(t)}) \end{bmatrix}$$

8) Compute the thermal power from the power balance constraint. The thermal power for particular iteration t and firefly F is given as follows:

$$\mathbf{P}_{TH\,(N_S\times 1)}^{(t)} = \mathbf{P}_{D(N_S\times 1)} + \mathbf{P}_{L\,(N_S\times 1)}^{(t)} - (\mathbf{P}_{S_{1,f}\,(N_s\times 1)} + \mathbf{P}_{S_{2,f}\,(N_s\times 1)} + \mathbf{P}_{S_{3,f}\,(N_s\times 1)} + \mathbf{P}_{H\,(N_S\times 1)}^{(t)})$$

where, transmission losses are determined as the function of the hydro power ($P_L = \mathbf{func}(P_H)$).

9) Find the thermal cost of the system corresponding to each firefly and check the thermal power limits. The total thermal cost of the system for particular firefly F and iteration t is given as follows:

$$C_F^{(t)} = \gamma \sum_{j=1}^{N_S} n_j P_{TH,j,F}^{2(t)} + \beta \sum_{j=1}^{N_S} n_j P_{TH,j,F}^{(t)} + \alpha \sum_{j=1}^{N_S} n_j$$

where, γ, β and α represent the cost coefficients of the thermal generation.
10) Compare the fireflies with each other based on their thermal cost and move the firefly having lower light intensity (higher fuel cost) towards a brighter firefly (lower fuel cost) using the multi-update criteria defined in Section 2 for the improved firefly algorithm. If the intensity of the particular firefly F is less than the firefly F', then the update equation is written as follows:

$$V_F^{(t+1)} = V_F^{(t)} + c_1\beta_o e^{-\delta R_{FF'}^2}(V_{F'}^{(t)} - V_F^{(t)}) + \alpha(rand - \frac{1}{2}) + c_2\beta_o e^{-\delta R_{Fg*}^2}(V_{g*}^{(t)} - V_F^{(t)})$$

If the intensity of the particular firefly F is greater than the firefly F', then the update equation is written as follows:

$$V_F^{(t+1)} = V_F^{(t)} + c_2\beta_o e^{-\delta R_{Fg*}^2}(V_{g*}^{(t)} - V_F^{(t)}) + \alpha(rand - \frac{1}{2})$$

11) Dynamically squeeze the maximum and minimum volume limits for each firefly.
12) Rank the fireflies and compute the updated global best firefly.
13) Repeat the steps (6)-(12) until the solution converges to the final value.
14) Find the total cost of the system using (29).

C. SIMULATION PARAMETERS

For simulating the different test cases, this section describes the essential system parameters of each energy source in the suggested hybrid system. The test cases are developed according to the parameters provided in [48].

TABLE 9. Load demand for different scheduling intervals for case 1.

Day	Scheduling Interval	Time (hrs)	Load Demand (MW)
Day 1	1	12:00 AM–12:00 PM	1200
	2	12:00 PM–12:00 AM	1500
Day 2	3	12:00 AM–12:00 PM	1100
	4	12:00 PM–12:00 AM	1800
Day 3	5	12:00 AM–12:00 PM	950
	6	12:00 PM–12:00 AM	1300

1) PARAMETERS FOR CASE 1

The cost equation for thermal generation for case 1 is given as follows:

$$F(P_{TH}) = 575 + 9.2P_{TH} + 0.00184P_{TH}^2 \quad (\$/hr) \quad (42)$$

where,

$$150\ MW \leq P_{TH} \leq 1500\ MW$$

In order to find the hydro power from the discharge rate, following discharge rate characteristics are used:

$$Dis(P_H) = 330 + 4.97P_H \quad (acre - ft/hr) \quad (43)$$

where,

$$0\ MW \leq P_H \leq 1000\ MW$$

The loss equation in order to find the transmission losses of the network is modeled as the function of the hydro power and is given as follows:

$$P_L = \mathbf{func}(P_H) = 0.00008P_H^2\ (MW) \quad (44)$$

The forecasted solar power for different scheduling intervals for case 1 is listed in Table 6. The different parameters for case 1 are listed in Table 8. The demand value for different scheduling intervals is given in Table 9.

2) PARAMETERS FOR CASE 2

For case 2, the cost equation for the thermal generation is given as follows:

$$F(P_{TH}) = 700 + 4,8P_{TH} + 0.0005P_{TH}^2 \quad (\$/hr) \quad (45)$$

where,

$$200\ MW \leq P_{TH} \leq 1200\ MW$$

In order to find the hydro power from the discharge rate, following discharge rate characteristics are used:

$$Dis(P_H) = 260 + 10P_H \quad (acre - ft/hr) \quad (46)$$

where,

$$0\ MW \leq P_H \leq 350\ MW$$

The loss equation in order to find the transmission losses of the network is modeled as the function of the hydro power and is given as follows:

$$P_L = \mathbf{func}(P_H) = 0.00008P_H^2\ (MW) \quad (47)$$

TABLE 10. Load demand for different scheduling intervals for case 2.

Day	Scheduling Interval	Time (hrs)	Load Demand (MW)
Day 1	1	12:00 AM–4:00 AM	600
	2	4:00 AM–8:00 AM	1000
Day 1	3	8:00 AM–12:00 PM	900
	4	12:00 PM–4:00 PM	500
Day 1	5	4:00 PM–8:00 PM	400
	6	8:00 PM–12:00 AM	500

The forecasted solar power for different scheduling intervals for case 1 is listed in Table 7. The different parameters for case 2 are listed in Table 8. The demand value for different scheduling intervals is given in Table 10.

D. RESULTS

This section covers the results of both cases, which includes the optimal power contribution of each energy source along with the analysis of the desired system parameters at the end of the scheduling problem. The test cases are solved using both conventional and dynamically search space squeezed modified firefly techniques while using different population size.

1) RESULTS OF CASE 1

The convergence characteristics are determined for case 1 using both conventional and modified firefly algorithms. Fig. 11 shows the convergence of the total fuel cost for case 1 using both techniques.

From the convergence graph, it is evident that the total fuel cost converges to a relatively lower value in case of the modified firefly algorithm as compared to the simple firefly. Fig. 12 shows the optimal contribution of each energy source for different scheduling intervals for both techniques. The optimal power contribution of different PV plants during various scheduling intervals is equal to the forecasted values given in Table 6. The cumulative sum of the power contribution of each energy source during a particular scheduling interval equals the sum of the demand value and the transmission losses for that interval.

Table 11 summarizes the results of the case 1 using the simple firefly technique for a population size of 5 fireflies. From Table 11, it is evident that the transmission losses depend upon the hydro power share for a particular scheduling interval. The greater the hydro power for a given interval, the more will be the network losses for that interval. Moreover, the ending volume for case 1 equals the desired value of 6000 acre-ft which satisfies the ending volume constraint of the reservoir. The hydro power, the solar power and the thermal power are within the defined limits as described in the previous section for each scheduling interval. The discharge rate for each interval is computed by using the equation of continuity while taking into account the two consecutive volume values. For interval 1, the initial volume of the reservoir is used for computing the discharge rate. Table 12 summarizes the results

TABLE 11. Complete results of case 1 using simple firefly algorithm for population size of 5 fireflies.

Interval Number	Load Demand (MW)	Losses (MW)	Reservoir Values		Solar Power Contribution (MW)			Power Contribution of Conventional Sources (MW)		Total Solar Cost ($)			Total Thermal Cost ($)	Total Generation Cost ($)
			Volume (acre-ft)	Discharge Rate (acre-ft/hr)	P_{S_1}	P_{S_2}	P_{S_3}	P_{TH}	P_H	C_1	C_2	C_3		
1	1200	39.5	78110	3824	25.00	11.47	0.229	499.8	703.34					
2	1500	12.6	74475	2302.9	59.30	27.35	0.546	1028.4	396.96					
3	1100	4.7	80098	1531.5	108.27	51.45	1.027	702.2	241.74	80200	47550	760	592570	721080
4	1800	9.6	79471	2052.2	204.89	98.14	1.961	1158.1	346.51					
5	950	8.3	80313	1929.9	89.67	42.23	0.843	503.6	321.90					
6	1300	36.6	**60000**	3692.8	181.21	86.33	1.725	390.7	676.61					

TABLE 12. Complete results of case 1 using modified firefly algorithm for population size of 5 fireflies.

Interval Number	Load Demand (MW)	Losses (MW)	Reservoir Values		Solar Power Contribution (MW)			Power Contribution of Conventional Sources (MW)		Total Solar Cost ($)			Total Thermal Cost ($)	Total Generation Cost ($)
			Volume (acre-ft)	Discharge Rate (acre-ft/hr)	P_{S_1}	P_{S_2}	P_{S_3}	P_{TH}	P_H	C_1	C_2	C_3		
1	1200	10.6	98286	2142.8	25.00	11.47	0.229	809.18	364.75					
2	1500	31.0	81213	3422.8	59.30	27.35	0.546	821.47	622.28					
3	1100	2.0	91759	1121.1	108.27	51.45	1.027	782.09	159.17	80200	47550	760	584800	713310
4	1800	35.7	71977	3648.6	204.89	98.14	1.961	862.95	667.71					
5	950	13.0	68002	2331.2	89.67	42.23	0.843	427.56	402.66					
6	1300	17.7	**60000**	2666.8	181.21	86.33	1.725	578.23	470.18					

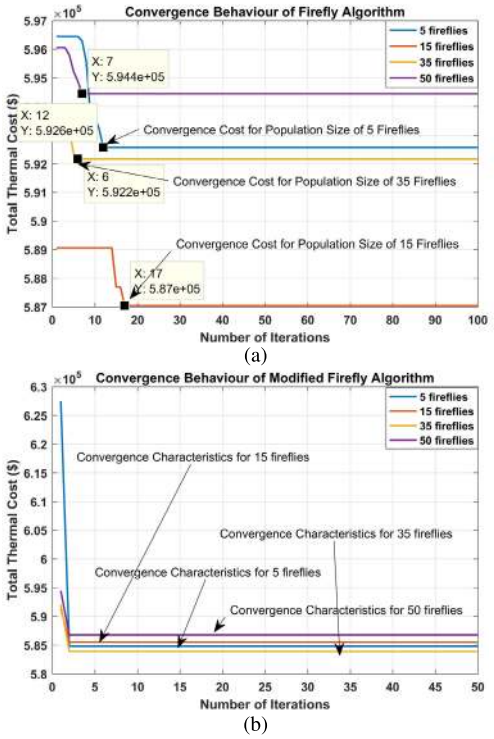

FIGURE 11. Convergence of the total thermal cost for case 1 using different techniques. (a) Simple firefly algorithm. (b) Modified firefly algorithm.

of case 1 using modified firefly algorithm for population size of 5 fireflies. From Table 12, it is clear that the suggested modified firefly technique converges to a lower thermal cost for this particular sample. The power limits constraint, the reservoir constraints and the power balance constraint are all satisfied for case 1 while using modified firefly technique.

The solar power share for different scheduling intervals and the total solar cost remain same for both techniques whereas the thermal cost converges to a lower value in case of modified firefly algorithm.

2) RESULTS OF CASE 2

Fig. 13 shows the convergence behavior of the simple firefly algorithm for case 2 using the different number of fireflies.

Fig. 14 shows the convergence behavior of the modified firefly algorithm for case 2 using the different number of fireflies. From both Fig. 13 and Fig. 14, it is evident that the modified firefly algorithm converges to a relatively lower fuel cost as compared to the simple firefly technique for different number of fireflies. The convergence behavior of the simple firefly algorithm in case of the population size of 5 fireflies is better than the modified firefly technique as evident from the graphs. Fig. 15 shows the optimal power contribution of different energy sources for each scheduling interval. Table 13 summarizes the results of conventional firefly technique for case 2. The final volume of the reservoir in this case equals the desired value of 12000 (acre-ft) and hence the final volume constraint is satisfied. The sum of the optimal power contribution of each energy source during the particular interval equals the demand plus the transmission losses for that interval. The discharge rate for each scheduling interval is computed by using the equation of continuity

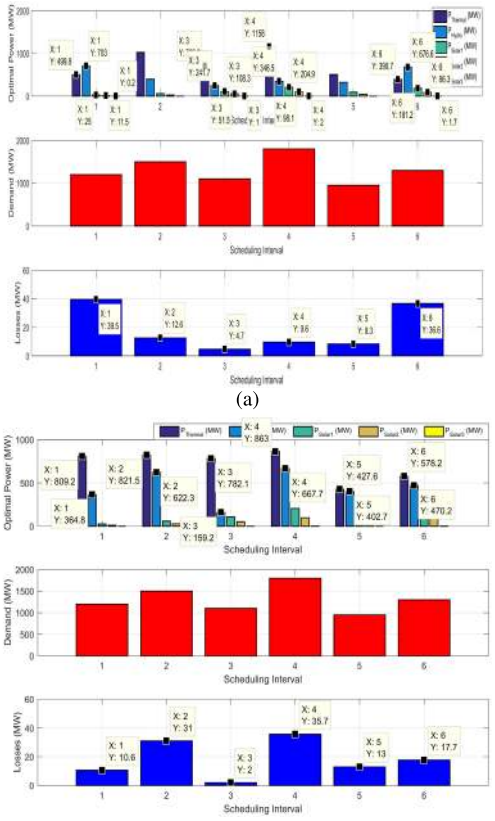

FIGURE 12. Optimal power contribution of each energy source for different scheduling intervals using both techniques. (a) Simple firefly algorithm. (b) Modified firefly algorithm.

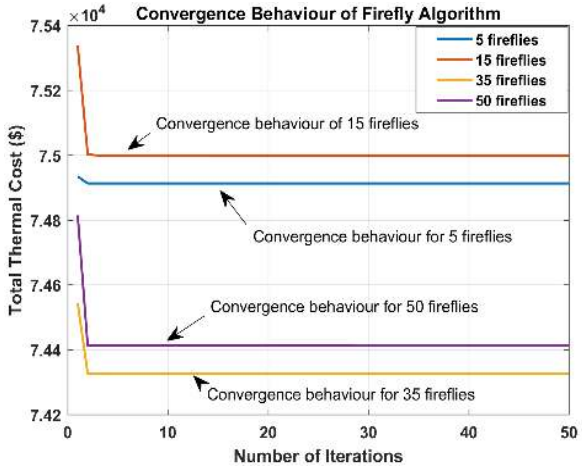

FIGURE 13. Convergence of the total thermal cost for case 2 using simple firefly.

as described previously. For interval 1, the initial volume of the reservoir is used for determining the discharge rate. The transmission losses depend upon the hydro power for particular scheduling interval.

Table 14 shows the complete results for case 2 using the modified firefly algorithm. The final volume constraint, the power limits constraint and the power balance constraint are all satisfied for case 2 while using the modified firefly algorithm. The solar cost remains constant for both techniques

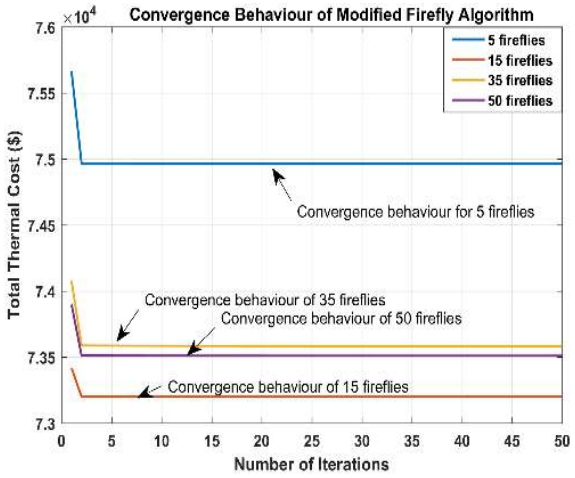

FIGURE 14. Convergence of the total thermal cost for case 2 using modified firefly.

while the total fuel cost converges to a lower value in case of the simple firefly algorithm for this particular sample. This completes the results of both cases using the simple and modified firefly algorithm. The next section introduces the statistical comparison of both techniques for each case in order to compare the performance parameters of the two algorithms statistically.

V. RESULTS OF STATISTICAL COMPARISON

The meta-heuristic algorithms have certain random part in their update criteria while shifting the possible solutions in the search space of the objective function. This results in the different final convergence results for each trial. Therefore, in order to compare the performance of a particular algorithm with the other, certain statistical measures are required to comprehensively compare both algorithms over a particular sample size. This research suggests the comparison of the average of two algorithms for different population sizes and then uses the independent t-test results to statistically prove the existence of the significant mean difference between the two techniques. The final comparison is made by taking into account both the average mean cost and the results of the independent t-test results. Moreover, the average generation cost for different number of fireflies is considered to be the final solution for the suggested algorithms for each case. In references [9]–[25], the authors compare the different techniques by comparing their mean cost. However, in majority references only a slight improvement in the mean cost is shown by the authors which is not statistically significant to prove the significance of the suggested technique. Therefore, while comparing different meta-heuristic methods, certain statistical methods should be used to statistically prove the significance of the suggested method. This research uses the independent t-test results to compare the mean and the variance of the algorithms statistically. The two major parts of the independent t-test results are the Levene's test for comparing the variance and the t-test for comparing the mean of the algorithms. For both Levene's and t-test results, if the

TABLE 13. Complete results of case 2 using simple firefly algorithm for population size of 5 fireflies.

Interval Number	Load Demand (MW)	Losses (MW)	Reservoir Values		Solar Power Contribution (MW)			Power Contribution of Conventional Sources (MW)		Total Solar Cost ($)			Total Thermal Cost ($)	Total Generation Cost ($)
			Volume (acre-ft)	Discharge Rate (acre-ft/hr)	P_{S_1}	P_{S_2}	P_{S_3}	P_{TH}	P_H	C_1	C_2	C_3		
1	600	0.1	13300	674.9	0.034	0.015	0.00031	558.59	41.48					
2	1000	1.1	15567	1433.3	0.040	0.018	0.00037	883.70	117.33					
3	900	2.9	14908	2164.8	24.92	11.44	0.022	676.03	190.47	10118	5825	9.0	74913	90865
4	500	2.5	14848	2014.9	44.07	20.33	0.040	262.52	175.48					
5	400	2.4	14928	1980.1	15.22	7.00	0.014	208.10	172.01					
6	500	4.9	**12000**	2732.0	0.017	0.008	0.00016	257.66	247.19					

TABLE 14. Complete results of case 2 using modified firefly algorithm for population size of 5 fireflies.

Interval Number	Load Demand (MW)	Losses (MW)	Reservoir Values		Solar Power Contribution (MW)			Power Contribution of Conventional Sources (MW)		Total Solar Cost ($)			Total Thermal Cost ($)	Total Generation Cost ($)
			Volume (acre-ft)	Discharge Rate (acre-ft/hr)	P_{S_1}	P_{S_2}	P_{S_3}	P_{TH}	P_H	C_1	C_2	C_3		
1	600	0.4	12160	960.1	0.034	0.015	0.00031	530.33	70.01					
2	1000	1.8	13122	1759.3	0.040	0.018	0.00037	851.80	149.93					
3	900	0.8	16127	1248.8	24.92	11.44	0.022	765.51	98.87	10118	5825	9.0	74966	90918
4	500	3.0	15297	2207.6	44.07	20.33	0.040	243.82	194.75					
5	400	2.4	15365	1982.9	15.22	7.00	0.014	207.83	172.29					
6	500	5.3	**12000**	2841.3	0.017	0.008	0.00016	247.17	258.12					

TABLE 15. Statistical comparison between firefly and modified firefly for case 1 using 30 samples.

Population Size	Average Cost ($)		Maximum Cost ($)		Minimum Cost ($)		Average Execution Time (sec)		Significant Values for Each Test	
	Firefly	Modified Firefly	Firefly	Modified Firefly	Firefly	Modified Firefly	Firefly	Modified Firefly	T-test	Levene's Test
5 Fireflies	713522	708829	726380	719660	700210	690420	0.957	0.948	0.024	0.015
15 Fireflies	707171	709785	717060	722350	700520	690280	0.985	0.977	0.012	0.009
35 Fireflies	711346	706055	723010	722350	700070	690280	1.05	1.12	0.028	0.02
50 Fireflies	713611	707491	722490	722350	701720	690280	1.20	1.18	0.031	0.08

TABLE 16. Statistical comparison between firefly and modified firefly for case 2 using 30 samples.

Population Size	Average Cost ($)		Maximum Cost ($)		Minimum Cost ($)		Average Execution Time (sec)		Significant Values for Each Test	
	Firefly	Modified Firefly	Firefly	Modified Firefly	Firefly	Modified Firefly	Firefly	Modified Firefly	T-test	Levene's Test
5 Fireflies	90046	89605	90890	90788	89186	89135	0.65	0.62	0.009	0.008
15 Fireflies	90074	89644	90866	90466	89250	89182	0.72	0.71	0.007	0.015
35 Fireflies	89976	89551	90837	90481	89233	89121	1.03	1.05	0.004	0.006
50 Fireflies	90278	89595	90866	90345	89186	89121	1.25	1.27	0.012	0.04

significant value is larger than the critical value of 0.05, the two algorithms have same variance and mean statistically for 95 % confidence level. Table 15 shows the comparison of the algorithms for case 1 using 30 samples. The algorithm is tested for different population sizes to increase the diversity of the fireflies and to suppress the effect of the premature convergence on the final converged solution. It is evident from the Table 15, that the suggested modified firefly algorithm outperforms the simple firefly by giving the lower mean generation cost and the execution time. Moreover, the significant values for both Levene's and the t-test are less than the critical value of 0.05 for majority of the cases, therefore the algorithms are statistically different from each other for case 1. Only for population size of 50 fireflies, the significant value for the Levene's test is greater than 0.05, which suggests that the two algorithms have same variance statistically for population size of 50 fireflies. Table 16 shows the comparison of the algorithms for case 2 using

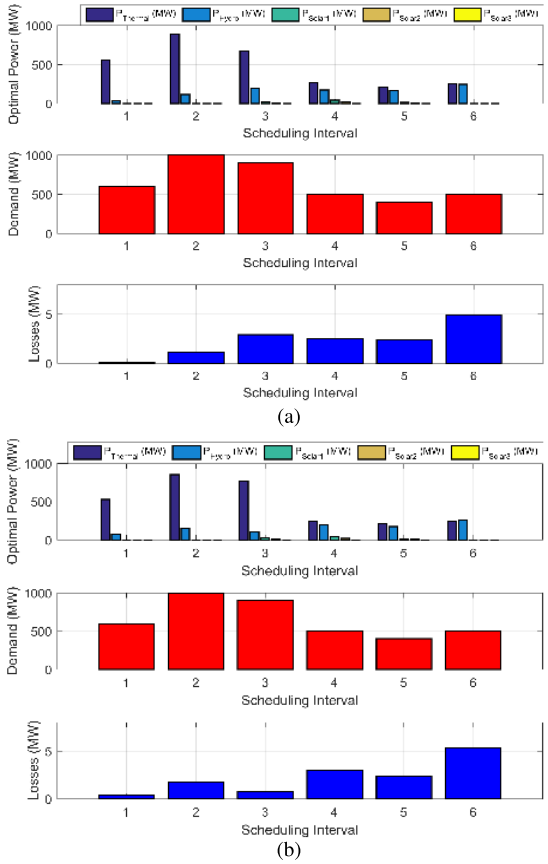

FIGURE 15. Optimal power contribution of each energy source for different scheduling intervals using both techniques for case 2. (a) Simple firefly algorithm. (b) Modified firefly algorithm.

30 samples. From Table 16, it is evident that the suggested firefly algorithm outperforms the simple firefly technique by giving lower generation cost and execution time. Moreover, the significant values for Levene's and t-test suggest that the two algorithms are statistically different from each other.

VI. COMPARISON WITH OTHER TECHNIQUES

The suggested modified firefly algorithm is compared with other promising techniques in literature to further validate its significance. The methods used for the comparison purpose are PSO, Accelerated PSO (APSO) and Improved Accelerated PSO (IAPSO). The mentioned methods are tested for the same problem under the same conditions and the results are shown in the Table 17. From Table 17, it is evident that the suggested firefly algorithm outperforms some other conventional and promising techniques in literature for the suggested hybrid system. The performance of suggested modified firefly is comparable with the conventional PSO, since PSO also depends upon both exploration and exploitation properties of the particles. The absence of the local search component in APSO and IAPSO results in relatively higher mean generation cost for this particular problem.

TABLE 17. Comparison between suggested firefly and different techniques for population size of 50 particles/fireflies.

Algorithm	Average Cost ($)	Maximum Cost ($)	Minimum Cost ($)	Average CPU time (sec)
Comparison for Case 1				
Modified Firefly	707491	722350	690280	1.18
APSO [48]	713874	722750	711690	1.32
IAPSO [48]	713587	722390	710480	1.35
PSO [49]	707736	724660	700500	1.52
Comparison for Case 2				
Modified Firefly	89595	90345	89121	1.27
APSO [48]	90716	90747	90698	1.20
IAPSO [48]	90712	90729	90695	1.26
PSO [49]	90168	90695	89705	1.48

VII. CONCLUSIONS, LIMITATIONS, AND FUTURE WORK

To summarize, following are the major findings of this research

1) This research suggests a modified dynamically search space squeezed firefly algorithm which uses multi-update criteria to shift the fireflies in the search space of the objective function by taking into account the influence of the global best solution for each iteration.
2) The proposed firefly technique is implemented on a novel dispatch problem which consists of a thermal unit, a hydroelectric energy source and multiple PV plants of different rated capacity. To model the intermittent nature of the PV source, combination of fractional integral polynomial method and ARIMA model is implemented to find the PV power share towards the dispatch problem.
3) The suggested firefly technique successfully solves a highly non-linear and multi-modal dispatch problem by giving the optimal power share of each energy source for different scheduling intervals.
4) Moreover, the performance of the two algorithms for different test cases is compared statistically using the independent t-test results. Based on the statistical analysis, the performance of the suggested modified firefly is enhanced by a substantial factor as compared to the simple firefly. The suggested technique proves to be optimal one for the given dispatch problem by giving lower generation cost and execution time.

Following are some of the practical limitations of the proposed research:

1) For photovoltaic system, the effect of the partial shading on the maximum power of the module is not considered extensively. The suggested system considers that each module is operating at maximum power point and there is only single global peak for the power curve.

2) The duration for which the forecasted parameters of the photovoltaic system remain constant is considered to be 1 hour. In practical scenarios, the irradiance and temperature levels can change with in the considered time duration.
3) Certain contingencies like removal of the transmission line, the removal of certain generating unit can affect the suggested operational strategy.
4) Resilience of the suggested system against the certain instabilities can improve the efficiency of the suggested dispatch strategy.

Based on the mentioned limitations, the future work involves the following major tasks:

1) Test the robustness of the suggested novel firefly technique on a more complex hybrid energy system while considering the security and emission constraints.
2) Model the power system to include the resilience against the disruptions to suggest a more practical operational strategy.
3) Consider the partial shading effect on the maximum power of the PV source. Decrease the time duration for which the forecasted parameters remain constant for the photovoltaic system.
4) Check the robustness of the suggested firefly algorithm on different forms of economic dispatch problems.

REFERENCES

[1] S. Fan, Z. Li, Z. Li, and G. He, "Evaluating and increasing the renewable energy share of Customers' electricity consumption," *IEEE Access*, vol. 7, pp. 129200–129214, 2019.
[2] M. B. Rasheed, M. A. Qureshi, N. Javaid, and T. Alquthami, "Dynamic pricing mechanism with the integration of renewable energy source in smart grid," *IEEE Access*, vol. 8, pp. 16876–16892, 2020.
[3] Y. Jia, Z. Y. Dong, C. Sun, and K. Meng, "Cooperation-based distributed economic MPC for economic load dispatch and load frequency control of interconnected power systems," *IEEE Trans. Power Syst.*, vol. 34, no. 5, pp. 3964–3966, Sep. 2019.
[4] T. G. Hlalele, R. M. Naidoo, J. Zhang, and R. C. Bansal, "Dynamic economic dispatch with maximal renewable penetration under renewable obligation," *IEEE Access*, vol. 8, pp. 38794–38808, 2020.
[5] W. Yi, Y. Zhang, Z. Zhao, and Y. Huang, "Multiobjective robust scheduling for smart distribution grids: Considering renewable energy and demand response uncertainty," *IEEE Access*, vol. 6, pp. 45715–45724, 2018.
[6] Y. Li, H. Tang, K. Lv, K. Wang, and G. Wang, "Optimization of dynamic dispatch for multiarea integrated energy system based on hierarchical learning method," *IEEE Access*, vol. 8, pp. 72485–72497, 2020.
[7] A. A. Hadi, C. A. S. Silva, E. Hossain, and R. Challoo, "Algorithm for demand response to maximize the penetration of renewable energy," *IEEE Access*, vol. 8, pp. 55279–55288, 2020.
[8] K. Tian, W. Sun, D. Han, and C. Yang, "Coordinated planning with predetermined renewable energy generation targets using extended two-stage robust optimization," *IEEE Access*, vol. 8, pp. 2395–2407, 2020.
[9] O. Hoseynpour, B. Mohammadi-Ivatloo, M. Nazari-Heris, and S. Asadi, "Application of dynamic non-linear programming technique to non-convex short-term hydrothermal scheduling problem," *Energies*, vol. 10, no. 9, p. 1440, Sep. 2017.
[10] S. Ghosh, M. Kaur, S. Bhullar, and V. Karar, "Hybrid ABC-BAT for solving short-term hydrothermal scheduling problems," *Energies*, vol. 12, no. 3, p. 551, Feb. 2019.
[11] C. Li, W. Wang, and D. Chen, "Multi-objective complementary scheduling of hydro-thermal-RE power system via a multi-objective hybrid grey wolf optimizer," *Energy*, vol. 171, pp. 241–255, Mar. 2019.
[12] M. Mohamed, A.-R. Youssef, S. Kamel, and M. Ebeed, "Lightning attachment procedure optimization algorithm for nonlinear non-convex short-term hydrothermal generation scheduling," *Soft Comput.*, vol. 24, no. 21, pp. 16225–16248, Nov. 2020.
[13] H. Yin, F. Wu, X. Meng, Y. Lin, J. Fan, and A. Meng, "Crisscross optimization based short-term hydrothermal generation scheduling with cascaded reservoirs," *Energy*, vol. 203, Jul. 2020, Art. no. 117822.
[14] Tehzeeb-ul-Hassan, T. Alquthami, S. E. Butt, M. F. Tahir, and K. Mehmood, "Short-term optimal scheduling of hydro-thermal power plants using artificial bee colony algorithm," *Energy Rep.*, vol. 6, pp. 984–992, Nov. 2020.
[15] J. Kong, H. I. Skjelbred, and O. B. Fosso, "An overview on formulations and optimization methods for the unit-based short-term hydro scheduling problem," *Electr. Power Syst. Res.*, vol. 178, Jan. 2020, Art. no. 106027.
[16] F. Zhu, P.-A. Zhong, B. Xu, W. Liu, W. Wang, Y. Sun, J. Chen, and J. Li, "Short-term stochastic optimization of a hydro-wind-photovoltaic hybrid system under multiple uncertainties," *Energy Convers. Manage.*, vol. 214, Jun. 2020, Art. no. 112902.
[17] A. S. Azad, M. S. A. Rahaman, J. Watada, P. Vasant, and J. A. G. Vintaned, "Optimization of the hydropower energy generation using meta-heuristic approaches: A review," *Energy Rep.*, vol. 6, pp. 2230–2248, Nov. 2020.
[18] Q. Tan, Y. Ding, Q. Ye, S. Mei, Y. Zhang, and Y. Wei, "Optimization and evaluation of a dispatch model for an integrated wind-photovoltaic-thermal power system based on dynamic carbon emissions trading," *Appl. Energy*, vol. 253, Nov. 2019, Art. no. 113598.
[19] X. Li, W. Wang, H. Wang, J. Wu, X. Fan, and Q. Xu, "Dynamic environmental economic dispatch of hybrid renewable energy systems based on tradable green certificates," *Energy*, vol. 193, Feb. 2020, Art. no. 116699.
[20] H. Yang, Q. Yu, J. Liu, Y. Jia, G. Yang, E. Ackom, and Z. Y. Dong, "Optimal wind-solar capacity allocation with coordination of dynamic regulation of hydropower and energy intensive controllable load," *IEEE Access*, vol. 8, pp. 110129–110139, 2020.
[21] V. K. Jadoun, V. C. Pandey, N. Gupta, K. R. Niazi, and A. Swarnkar, "Integration of renewable energy sources in dynamic economic load dispatch problem using an improved fireworks algorithm," *IET Renew. Power Gener.*, vol. 12, no. 9, pp. 1004–1011, Jul. 2018.
[22] S. A. Alavi, A. Ahmadian, and M. Aliakbar-Golkar, "Optimal probabilistic energy management in a typical micro-grid based-on robust optimization and point estimate method," *Energy Convers. Manage.*, vol. 95, pp. 314–325, May 2015.
[23] M. Xie, S. Ke, J. Xiong, P. Cheng, and M. Liu, "Recursive dynamic regression-based two-stage compensation algorithm for dynamic economic dispatch considering high-dimensional correlation of multi-wind farms," *IET Renew. Power Gener.*, vol. 13, no. 3, pp. 475–481, Feb. 2019.
[24] J. He, Z. Yuan, X. Yang, W. Huang, Y. Tu, and Y. Li, "Reliability modeling and evaluation of urban multi-energy systems: A review of the state of the art and future challenges," *IEEE Access*, vol. 8, pp. 98887–98909, 2020.
[25] M. Basu, "Combined heat and power dynamic economic dispatch with demand side management incorporating renewable energy sources and pumped hydro energy storage," *IET Gener., Transmiss. Distrib.*, vol. 13, no. 17, pp. 3771–3781, Sep. 2019.
[26] S. Liaquat, M. S. Fakhar, S. A. R. Kashif, A. Rasool, O. Saleem, and S. Padmanaban, "Performance analysis of APSO and firefly algorithm for short term optimal scheduling of multi-generation hybrid energy system," *IEEE Access*, vol. 8, pp. 177549–177569, 2020.
[27] B. Khan and P. Singh, "Selecting a meta-heuristic technique for smart micro-grid optimization problem: A comprehensive analysis," *IEEE Access*, vol. 5, pp. 13951–13977, 2017.
[28] Y. Yang, B. Wei, H. Liu, Y. Zhang, J. Zhao, and E. Manla, "Chaos firefly algorithm with self-adaptation mutation mechanism for solving large-scale economic dispatch with valve-point effects and multiple fuel options," *IEEE Access*, vol. 6, pp. 45907–45922, 2018.
[29] C. Gerez, L. I. Silva, E. A. Belati, A. J. S. Filho, and E. C. M. Costa, "Distribution network reconfiguration using selective firefly algorithm and a load flow analysis criterion for reducing the search space," *IEEE Access*, vol. 7, pp. 67874–67888, 2019.
[30] M. Zhang, Z. Chen, and L. Wei, "An immune firefly algorithm for tracking the maximum power point of PV array under partial shading conditions," *Energies*, vol. 12, no. 16, p. 3083, Aug. 2019.
[31] S. Liaquat, O. Saleem, and K. Azeem, "Comparison of firefly and hybrid firefly-APSO algorithm for power economic dispatch problem," in *Proc. Int. Conf. Technol. Policy Energy Electr. Power (ICT-PEP)*, Bandung, Indonesia, Sep. 2020, pp. 94–99.

[32] X. S. Yang, "Firefly algorithm," in *Engineering Optimization: An Introduction with Metaheuristic Applications*, 2nd ed. Hoboken, NJ, USA: Wiley, 2010, ch. 17, sec. 2, pp. 221–229.
[33] S. L. Tilahun, J. M. T. Ngnotchouye, and N. N. Hamadneh, "Continuous versions of firefly algorithm: A review," *Artif. Intell. Rev.*, vol. 51, no. 3, pp. 445–492, Mar. 2019.
[34] P. Kora and K. S. R. Krishna, "Hybrid firefly and particle swarm optimization algorithm for the detection of bundle branch block," *Int. J. Cardiovascular Acad.*, vol. 2, no. 1, pp. 44–48, Mar. 2016.
[35] I. B. Aydilek, "A hybrid firefly and particle swarm optimization algorithm for computationally expensive numerical problems," *Appl. Soft Comput.*, vol. 66, pp. 232–249, May 2018.
[36] A. K. Barisal, "Dynamic search space squeezing strategy based intelligent algorithm solutions to economic dispatch with multiple fuels," *Int. J. Electr. Power Energy Syst.*, vol. 45, no. 1, pp. 50–59, Feb. 2013.
[37] X. Zhang, H. Liu, and L. Tu, "A modified particle swarm optimization for multimodal multi-objective optimization," *Eng. Appl. Artif. Intell.*, vol. 95, Oct. 2020, Art. no. 103905.
[38] L. Li, G. Li, and L. Chang, "A many-objective particle swarm optimization with grid dominance ranking and clustering," *Appl. Soft Comput.*, vol. 96, Nov. 2020, Art. no. 106661.
[39] Y. Mahmoud and E. El-Saadany, "Accuracy improvement of the ideal PV model," *IEEE Trans. Sustain. Energy*, vol. 6, no. 3, pp. 909–911, Jul. 2015.
[40] A. K. Panchal, "I–V data operated high-quality photovoltaic solution through per-unit single-diode model," *IEEE J. Photovolt.*, vol. 10, no. 4, pp. 1175–1184, Jul. 2020.
[41] E. I. Ortiz-Rivera, "Approximation of a photovoltaic module model using fractional and integral polynomials," in *Proc. 38th IEEE Photovoltaic Spec. Conf.*, Austin, TX, USA, Jun. 2012, pp. 002927–002931.
[42] M. Khashei, M. Bijari, and S. R. Hejazi, "Combining seasonal ARIMA models with computational intelligence techniques for time series forecasting," *Soft Comput.*, vol. 16, no. 6, pp. 1091–1105, Jun. 2012.
[43] K. Yunus, T. Thiringer, and P. Chen, "ARIMA-based frequency-decomposed modeling of wind speed time series," *IEEE Trans. Power Syst.*, vol. 31, no. 4, pp. 2546–2556, Jul. 2016.
[44] P. S. Paretkar, L. Mili, V. Centeno, K. Jin, and C. Miller, "Short-term forecasting of power flows over major transmission interties: Using box and Jenkins ARIMA methodology," in *Proc. IEEE PES Gen. Meeting*, Providence, RI, USA, Jul. 2010, pp. 25–29.
[45] A. Andreas and S. Wilcox. *Solar Resource and Meteorological Assessment Project (SOLRMAP): Rotating Shadowband Radiometer (RSR); Los Angeles, California (Data)*. Accessed: 2012. [Online]. Available: http://dx.doi.org/10.5439/1052230
[46] J. J. Chen and J. H. Zheng, "'Discussion on 'Short-term environmental/economic hydrothermal scheduling,'" *Electr. Power Syst. Res.*, vol. 127, pp. 348–350, Oct. 2015.
[47] H. Zhang, J. Zhou, Y. Zhang, N. Fang, and R. Zhang, "Short term hydrothermal scheduling using multi-objective differential evolution with three chaotic sequences," *Int. J. Electr. Power Energy Syst.*, vol. 47, pp. 85–99, May 2013.
[48] M. S. Fakhar, S. A. R. Kashif, N. U. Ain, H. Z. Hussain, A. Rasool, and I. A. Sajjad, "Statistical performances evaluation of APSO and improved APSO for short term hydrothermal scheduling problem," *Appl. Sci.*, vol. 9, no. 12, p. 2440, Jun. 2019.
[49] B. Yu, X. Yuan, and J. Wang, "Short-term hydro-thermal scheduling using particle swarm optimization method," *Energy Convers. Manage.*, vol. 48, no. 7, pp. 1902–1908, Jul. 2007.

SHEROZE LIAQUAT received the bachelor's and master's degree in electrical engineering with specialization in power systems from the University of Engineering and Technology, Lahore, Pakistan, in 2018 and 2020, respectively. He is currently serving as a Faculty Member with the Electrical Engineering Department, National University of Computer and Emerging Sciences, Lahore. His current research interests include the application of meta-heuristic techniques, soft computing methods, and machine learning algorithms in the economic dispatch problems of hybrid energy systems under the penetration of distributed generation sources.

MUHAMMAD SALMAN FAKHAR received the bachelor's and master's degrees in electrical engineering with specialization in power systems from the University of Engineering and Technology (U.E.T), Lahore, Pakistan, where he is currently pursuing the Ph.D. degree with specialization in the design of novel meta-heuristic algorithms for variants of short term hydrothermal scheduling problem. He is also serving as a Lecturer with the Electrical Engineering Department, UET. His current research interests include the application of meta-heuristic techniques and their variants for optimal scheduling of conventional sources and the investigation of short-term hydro thermal scheduling problem.

SYED ABDUL RAHMAN KASHIF received the B.Sc., M.Sc., and Ph.D. degrees in electrical engineering from the University of Engineering and Technology (U.E.T), Lahore, Pakistan. He is currently serving as an Associate Professor for the Department of Electrical Engineering, UET. His research interests include power electronics, control of electrical machines, smart grids, and application of neural networks and fuzzy techniques in power engineering.

AKHTAR RASOOL received the B.Sc. and M.Sc. degree in electrical engineering in 2007 and 2009, respectively, and the Ph.D. degree in mechatronics engineering with thesis title, Control of Converters as Source for Microgrid, in 2017. He has been serving as an Assistant Professor and the Director for Quality Enhancement Cell, Sharif College of Engineering and Technology, Lahore (Affiliated with the College of University of Engineering and Technology, Lahore) since April 2018. Earlier, he has served as an Assistant Professor for the University of Engineering and Technology, Taxila, till April 2018, a Teaching Assistant for Sabanci University, till July 2017, a Lecturer for Hajvery University, till 2012, and a Lab Engineer for Government College University Faisalabad, till January 2008. Beside the academic roles, he has also served a vast range for industries through services and consultancy firms, PRESCON Engineering (Pvt.,) Ltd., Orient Energy Systems (Pvt.,) Ltd., and AGITROL Solution (Pvt.,) Ltd. His major areas of research interest include control of converters with applications ranging integration of renewable energy resources, microgrids, smartgrids, electrical machines, automated electrical vehicles, electrical trains, automatic braking, steering, robotic actuators, energy management, process control, cascaded control applications, high-voltage assets' life assessment, and artificial intelligence. He is also actively involved in training for the Quality Enhancement, Objectives Based Education (OBE), and Objectives Based Assessment (OBA) techniques. He is also serving as an Associate Editor for *World Journal of Engineering*, an Editorial Advisory Member for *International Journal of Electrical Engineering and Computing*, and *LC International Journal of STEM* beside reviewing for many prestigious journals from IEEE, IET, Elsevier, and other publishers, including IEEE TRANSACTIONS ON ENERGY CONVERSION, IEEE TRANSACTIONS ON POWER SYSTEMS, *IET Power Electronics*, *Energy Reports*, and among others.

OMER SALEEM received the bachelor's and master's degrees in electrical engineering with specialization in control systems from the University of Engineering and Technology (U.E.T.), Lahore, Pakistan, where he is currently pursuing the Ph.D. degree with specialization in adaptive control systems. He is also serving as an Assistant Professor for the Department of Electrical Engineering, National University of Computer and Emerging Sciences, Lahore. His research interests include the design of adaptive and self-tuning control systems for mechatronic systems, and power electronic converters.

MUHAMMAD FAHAD ZIA (Member, IEEE) received the B.Sc. degree (Hons.) in electrical engineering from the University of Engineering and Technology, Lahore, Pakistan, the M.S. degree in electrical engineering from the King Fahd University of Petroleum and Minerals, Dhahran, Saudi Arabia, and the Ph.D. degree in electrical engineering from the University of Brest, Brest, France, in 2020.

He is currently working as an Assistant Professor with the Department of Electrical Engineering, National University of Computer and Emerging Sciences, Pakistan. His main research interests and experience include AC/DC microgrids, energy management system, transactive energy, power system operation, and power electronics. He is also serving as a Reviewer for many prestigious journals from IEEE, IET, and other publishers, including IEEE TRANSACTIONS ON SMART GRID, IEEE TRANSACTIONS ON SYSTEMS, MAN, AND CYBERNETICS: SYSTEMS, *IET Renewable Power Generation*, *IET Generation, Transmission, and Distribution*, and among others.

SANJEEVIKUMAR PADMANABAN (Senior Member, IEEE) received the bachelor's degree in electrical engineering from the University of Madras, Chennai, India, in 2002, the master's degree (Hons.) in electrical engineering from Pondicherry University, Puducherry, India, in 2006, and the Ph.D. degree in electrical engineering from the University of Bologna, Bologna, Italy, in 2012.

He was an Associate Professor with VIT University from 2012 to 2013. In 2013, he joined the National Institute of Technology, India, as a Faculty Member. In 2014, he was invited as a Visiting Researcher with the Department of Electrical Engineering, Qatar University, Doha, Qatar, funded by the Qatar National Research Foundation (Government of Qatar). He continued his research activities with the Dublin Institute of Technology, Dublin, Ireland, in 2014. Further, he served an Associate Professor for the Department of Electrical and Electronics Engineering, University of Johannesburg, Johannesburg, South Africa, from 2016 to 2018. Since 2018, he has been a Faculty Member with the Department of Energy Technology, Aalborg University, Esbjerg, Denmark. He has authored more than 300 scientific articles. He is a Fellow of the Institution of Engineers, India, the Institution of Electronics and Telecommunication Engineers, India, and the Institution of Engineering and Technology, U.K. He was a recipient of the Best Paper cum Most Excellence Research Paper Award from IET-SEISCON'13, IET-CEAT'16, IEEE-EECSI'19, IEEE-CENCON'19, and five best paper awards from ETAEERE'16 sponsored *Lecture Notes in Electrical Engineering* (Springer). He is an Editor/Associate Editor/Editorial Board of refereed journals, in particular the IEEE SYSTEMS JOURNAL, IEEE TRANSACTION ON INDUSTRY APPLICATIONS, IEEE ACCESS, *IET Power Electronics*, *IET Electronics Letters*, and *International Transactions on Electrical Energy Systems* (Wiley), a Subject Editorial Board Member of *Energy Sources-Energies Journal*, MDPI, and the Subject Editor of the *IET Renewable Power Generation*, *IET Generation, Transmission, and Distribution*, and *FACTS Journal* (Canada).